



- (51) International Patent Classification:
H04B 1/16 (2006.01) H04W 52/02 (2009.01)
H04L 27/06 (2006.01)
- (21) International Application Number:
PCT/US2020/012439
- (22) International Filing Date:
06 January 2020 (06.01.2020)
- (25) Filing Language: English
- (26) Publication Language: English
- (30) Priority Data:
62/788,657 04 January 2019 (04.01.2019) US
- (71) Applicant: THE TRUSTEES OF COLUMBIA UNIVERSITY IN THE CITY OF NEW YORK [US/US]; 110 Low Memorial Library, 535 West 116th Street, New York, NY 10027 (US).
- (72) Inventors: MANGAL, Vivek; 3419 Vanderbilt Way, Santa Clara, CA 95051 (US). KINGET, Peter R.; 11 Franklin Place, Summit, NJ 07901 (US).
- (74) Agent: BYRNE, Matthew T. et al.; Byrne Poh LLP, 11 Broadway, Suite 760, New York, NY 10004 (US).
- (81) Designated States (unless otherwise indicated, for every kind of national protection available): AE, AG, AL, AM, AO, AT, AU, AZ, BA, BB, BG, BH, BN, BR, BW, BY, BZ, CA, CH, CL, CN, CO, CR, CU, CZ, DE, DJ, DK, DM, DO, DZ, EC, EE, EG, ES, FI, GB, GD, GE, GH, GM, GT, HN, HR, HU, ID, IL, IN, IR, IS, JO, JP, KE, KG, KH, KN, KP, KR, KW, KZ, LA, LC, LK, LR, LS, LU, LY, MA, MD, ME, MG, MK, MN, MW, MX, MY, MZ, NA, NG, NI, NO, NZ, OM, PA, PE, PG, PH, PL, PT, QA, RO, RS, RU, RW, SA, SC, SD, SE, SG, SK, SL, ST, SV, SY, TH, TJ, TM, TN, TR, TT, TZ, UA, UG, US, UZ, VC, VN, WS, ZA, ZM, ZW.
- (84) Designated States (unless otherwise indicated, for every kind of regional protection available): ARIPO (BW, GH,

(54) Title: CIRCUITS AND METHODS FOR WAKE-UP RECEIVERS

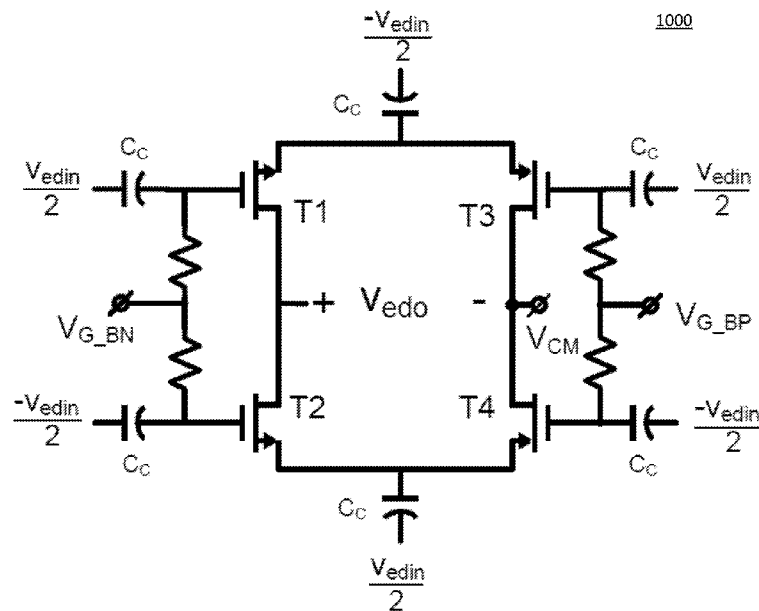


FIG. 10

(57) Abstract: Circuit for wake-up receivers are provide. In some embodiments, the wake-up receivers include self-mixers that receive a gate bias voltage. Some of the self-mixers are single ended and some are differential. In some embodiments, the wake-up receivers include a matching network that is connected to the input of the self-mixer. In some embodiments, the wake-up receivers include a low frequency path connected to the output of the self-mixer. In some embodiments, the wake-up receivers include a high frequency path connected to the output of the self-mixer. In some embodiments, the wake-up receivers are configured to receive an encoded bit stream. In some embodiments, the wake-up receivers are configured to wake-up another receiver.



GM, KE, LR, LS, MW, MZ, NA, RW, SD, SL, ST, SZ, TZ, UG, ZM, ZW), Eurasian (AM, AZ, BY, KG, KZ, RU, TJ, TM), European (AL, AT, BE, BG, CH, CY, CZ, DE, DK, EE, ES, FI, FR, GB, GR, HR, HU, IE, IS, IT, LT, LU, LV, MC, MK, MT, NL, NO, PL, PT, RO, RS, SE, SI, SK, SM, TR), OAPI (BF, BJ, CF, CG, CI, CM, GA, GN, GQ, GW, KM, ML, MR, NE, SN, TD, TG).

Published:

- *with international search report (Art. 21(3))*
- *before the expiration of the time limit for amending the claims and to be republished in the event of receipt of amendments (Rule 48.2(h))*

CIRCUITS AND METHODS FOR WAKE-UP RECEIVERS

Cross Reference to Related Application

[0001] This application claims the benefit on United States Provisional Patent Application No. 62/788,657, filed January 4, 2019, which is hereby incorporated by reference herein in its entirety.

Statement Regarding Government Funded Research

[0002] This invention was made with government support under 1309721 awarded by the National Science Foundation. The government has certain rights in the invention.

Background

[0003] In many energy-limited wireless communications applications, it is desirable for receivers to operate in a deep sleep mode when inactive to prolong lifetime on available power (e.g., such as power stored in a connected battery or other power source (e.g., a capacitor)).

[0004] One technique that can be used to enable the receivers to timely receive asynchronous communications is to use a first always ON (or almost always ON) (when in deep sleep mode) low-power receiver to receive a wake-up signal and, in response, turn ON a second main receiver. Such first receivers can be referred to herein as wake-up receivers.

[0005] Accordingly, new mechanisms for wake-up receivers are desirable.

Summary

[0006] In accordance with some embodiments, circuits and methods for wake-up receivers are provided. In some embodiments, circuits for wake-up receivers are provided, the circuits comprising: a first self-mixer stage comprising: a first NMOS transistor having a source, a drain, and a gate; a second NMOS transistor having a source, a drain, and a gate, wherein the drain of the second NMOS transistor is connected to the drain of the first NMOS transistor; a first PMOS transistor having a source, a drain, and a gate, wherein the source of the first PMOS transistor is connected to the source of the first NMOS transistor; a second PMOS transistor having a source, a drain, and a gate, wherein the drain of the second PMOS transistor is connected to the drain of the first PMOS transistor, and the source of the second PMOS transistor is connected to the source of the second NMOS transistor; a first resistor having a first side connected to the gate of the first NMOS transistor and having a second side connected to a first gate bias voltage; a second resistor having a first side connected to the gate of the first PMOS transistor and having a second side connected to a second gate bias voltage; a third resistor having a first side connected to the gate of the second NMOS transistor and having a second side connected to the first gate bias voltage; a fourth resistor having a first side connected to the gate of the second PMOS transistor and having a second side connected to the second gate bias voltage; a first coupling capacitor having a first side connected to a first radio frequency (RF) input signal and having a second side connected to the gate of the first NMOS transistor; a second coupling capacitor having a first side connected to the first RF input signal and having a second side connected to the gate of the first PMOS transistor; a third coupling capacitor having a first side connected to a second RF input signal and having a second side connected to the gate of the second NMOS

transistor; and a fourth coupling capacitor having a first side connected to the second RF input signal and having a second side connected to the gate of the second PMOS transistor.

Brief Description of the Drawings

[0007] Various objects, features, and advantages of the disclosed subject matter can be more fully appreciated with reference to the following detailed description of the disclosed subject matter when considered in connection with the following drawings, in which like reference numerals identify like elements.

[0008] FIG. 1 is an example of a single transistor self-mixer in accordance with some embodiments.

[0009] FIG. 2A is an example of an equivalent small-signal model of the circuit in FIG. 1 at an RF input frequency in accordance with some embodiments.

[0010] FIG. 2B is an example of an equivalent small-signal model of the circuit in FIG. 1 at a baseband frequency in accordance with some embodiments.

[0011] FIG. 3 is an example of a small signal model for ideal wake-up receiver front end in accordance with some embodiments.

[0012] FIG. 4 is an example of a graph showing that the input resistance $R_{in,ed}$ and input capacitance $C_{in,ed}$ of a self-mixer can be changed by changing V_{G_B} in accordance with some embodiments.

[0013] FIG. 5 is an example of a graph showing that varying V_{G_B} between 0.0 VDC and 0.3 VDC results in almost the same output from a self-mixer in accordance with some embodiments.

[0014] FIG. 6A is an example of a single-ended multi-transistor self-mixer in accordance with some embodiments.

[0015] FIG. 6B is an example of the operation of a transistor of the single-ended multi-transistor self-mixer of FIG. 6A when in a first configuration in accordance with some embodiments.

[0016] FIG. 6C is an example of the operation of a transistor of the single-ended multi-transistor self-mixer of FIG. 6A when in a second configuration in accordance with some embodiments.

[0017] FIG. 7A is an example of a small-signal model at RF of the circuit in FIG. 6A in accordance with some embodiments.

[0018] FIG. 7B is an example of a small-signal models at baseband frequency of the circuit in FIG. 6A in accordance with some embodiments.

[0019] FIG. 8 is an example of a one-transistor, differential self-mixer in accordance with some embodiments.

[0020] FIG. 9 is an example of an equivalent small-signal model at baseband of the circuit of FIG. 8 in accordance with some embodiments.

[0021] FIG. 10 is an example of a complete stage of a differential self-mixer combining a PMOS transistor pair and an NMOS transistor pair in accordance with some embodiments.

[0022] FIG. 11 is an example of a small-signal equivalent model of the circuit in FIG. 10 in accordance with some embodiments.

[0023] FIG. 12 is an example of a differential multi-stage self-mixer in accordance with some embodiments.

[0024] FIG. 13 is an example of a bias generator in accordance with some embodiments.

[0025] FIG. 14 is an example of a wake-up receiver architecture in accordance with some embodiments.

[0026] FIG. 15 is an example of an implementation of a self-mixer and a baseband amplifier in accordance with some embodiments.

[0027] FIG. 16 is an example of a detailed schematic of a wake-up receiver in accordance with some embodiments.

[0028] FIG. 17 is an example of a timing diagram in accordance with some embodiments.

[0029] FIG. 18 is an example of a multi-domain model of a wake-up receiver in accordance with some embodiments.

[0030] FIG. 19 is an example of a receiver having a low frequency path and a high frequency path that can be used to account for an interferer in accordance with some embodiments.

[0031] FIG. 20 is an example of a diagram illustrating how an interferer impacts a receiver having a self-mixer in accordance with some embodiments.

[0032] FIG. 21 is an example of another diagram illustrating how an interferer impacts a receiver having a self-mixer in accordance with some embodiments.

[0033] FIG. 22 is an example of a drawing showing how a transmitted signal can be impacted by an interferer in a receiver in accordance with some embodiments.

[0034] FIG. 23 is an example of an architecture for a self-mixer, a low-frequency path, and a high-frequency path of a wake-up receiver in accordance with some embodiments.

[0035] FIG. 24 is an example of an amplifier in accordance with some embodiments.

[0036] FIG. 25 is an example of a low-pass filter in accordance with some embodiments.

[0037] FIG. 26 is an example of a high-pass filter in accordance with some embodiments.

[0038] FIG. 27 is an example of an architecture for a wake-up receiver that can account for multiple interferers in accordance with some embodiments.

Detailed Description

[0039] As shown in FIG. 1, in accordance with some embodiments, a gate-biased self-mixer 100 is provided. As illustrated, self-mixer 100 includes an NMOS FET 102, an AC coupling capacitor C_C 104, a load capacitor C_L 106, and a bias resistor 108 in some embodiments.

[0040] During operation, in some embodiments, a DC gate bias potential, V_{G_B} , is provided at the gate of NMOS FET 100 via resistor 108 from terminal 110. This gate bias potential slightly forward biases the channel of NMOS FET 100, while still operating the transistor in the weak-inversion, linear region in some embodiments. The input signal, V_{edin} , is provided to self-mixer 100 at terminal 112, and an output signal, V_{edo} , is sensed from self-mixer 100 at terminal 114, in some embodiments.

[0041] FIG. 2A shows an example equivalent small-signal model 200 of the circuit in FIG. 1 at an RF input frequency, assuming capacitors C_C 104 and C_L 106 are sufficiently large to act as shorts at the operating radio frequency (RF).

[0042] FIG. 2B shows an example equivalent small-signal model 250 of the circuit in FIG. 1 at a baseband frequency, assuming capacitors C_C 104 and C_L 106 are sufficiently small to act as opens at the baseband frequency.

[0043] In some embodiments, self-mixer 100 (and other self-mixers as described herein) can be used to implement an energy detector.

[0044] FIG. 3 shows an example 300 of a small signal model for ideal receiver front end including an antenna 302, a matching network 304, and an energy detector 306. In this figure, antenna 302 is represented as a voltage source with a source resistance R_S of 50Ω and is matched to energy detector 306 using matching network 304, which has a passive gain A_v at frequency f_{rf} . Energy detector 306 has an input resistance $R_{in,ed}$, an input capacitance C_{in} , and a conversion gain constant k_{ed} . The passive gain A_v of the matching network causes V_{edin} to equal $V_{in}A_v$. The

passive gain A_v from matching network 304 at an angular frequency $\omega_{RF} = 2\pi f_{rf}$ can be written as:

$$A_v = \sqrt{\frac{R_{in,ed}}{R_s}} \left/ \sqrt{\left(1 + \frac{\omega_{RF} R_{in,ed} C_{in}}{Q_{ind}}\right)} \right.$$

wherein Q_{ind} is the quality factor of inductance L_{ind} of matching network 304. As can be seen from this equation, reducing the size of C_{in} can be used to increase the size of A_v , in some embodiments. Thus, a minimal C_{in} may be desirable in some embodiments.

[0045] In some embodiments, it is desirable to provide an input resistance $R_{in,ed}$ having a given value $R_{in,opt}$ that optimizes the sensitivity of energy detector 306. In some embodiments, $R_{in,opt}$ can be calculated as follows: $R_{in,opt} = Q_{ind}/\omega_{RF}C_{in}$. For example, for a Q_{ind} of 80, and a C_{in} of 1pF at a ω_{RF} of 434MHz, $R_{in,opt}$ (and thus $R_{in,ed}$) can have a value of 30k Ω , in some embodiments.

[0046] In some embodiments, the input capacitance C_{in} for self-mixer 100 may be dominated by the gate-to-source capacitance c_{gs} of transistor 102. Using a minimum-sized transistor for transistor 102 can keep C_{in} low. For example, in some embodiments, a transistor with a width W of 1 μm and a length of 60 nm may only contribute a capacitance of 1 fF.

[0047] As shown in FIG. 4, an example of a graph 400 showing that the input resistance $R_{in,ed}$ (or r_o as shown in FIG. 2) (shown by line 402) and input capacitance $C_{in,ed}$ (which may be dominated by c_{gs} as described above) (shown by line 404) of self-mixer 100 can be changed by changing V_{G_B} , in accordance with some embodiments. The particular values shown in FIG. 4 are for an example one-stage self-mixer including a single transistor with a channel width (W) of 1 μm and a channel length (L) of 60 nm in a 65 nm LP CMOS process. Other values may be

realized in some embodiments. In some embodiments, $R_{in,ed}$ can be a function of various parameters as follows:

$$R_{in,ed} = r_o = \frac{V_t}{K} = \frac{V_t L}{I_s W} e^{-V_{G_B}/(nV_t)}$$

wherein V_t (which is equal to $k_B T/q$) is the thermal voltage of transistor 102, k_B is the Boltzmann constant, T is absolute temperature of transistor 102, q is elementary charge, K equals $I_s(W/L)$, I_s is the saturation current of transistor 102, and n is the subthreshold-slope coefficient.

[0048] Turning to FIG. 5, an example of a graph 500 showing that varying V_{G_B} between 0.0 VDC and 0.3 VDC results in almost the same output (for a 5 mV peak RF input) (as shown by line 502) from self-mixer 100. Thus, V_{G_B} can be varied in this range to change the input resistance R_{edin} of self-mixer 100 (as shown by line 402 of FIG. 4) without changing the input capacitance (C_m) or gain of self-mixer 100 (as shown by line 504 of FIG. 5), in some embodiments.

[0049] Since the transistor is operating in the weak-inversion, linear region between 0.0 VDC and 0.3 VDC, the power spectral density (PSD) of the output noise of the self-mixer can be written as $4k_B T R_{out,ed}$, where $R_{out,ed}$ is equal to the channel resistance r_o for a one-stage self-mixer, such as self-mixer 100. FIG. 5 also shows an exponential drop in PSD at 100Hz for self-mixer 100 with increasing V_{G_B} , demonstrating the direct dependence of PSD on the channel resistance r_o .

[0050] Therefore, by increasing V_{G_B} within the weak-inversion, linear region, the self-mixer noise contribution at baseband can be reduced while keeping the conversion gain constant (or nearly constant) and the input capacitance low in order to maximize the signal-to-noise ratio (SNR) at the output of the self-mixer.

[0051] In some embodiments, further sensitivity enhancement can be achieved by increasing the conversion gain constant k_{ed} for the self-mixer.

[0052] Turning to FIG. 6A, an example 600 of a single-ended multi-transistor self-mixer in accordance with some embodiments is illustrated. As shown, self-mixer 600 includes NMOS FETs 602, 604, 606, and 608, coupling capacitors 610, 612, and 614, load capacitors 616 and 618, and a bias resistor 620.

[0053] Like self-mixer 100, during operation, a gate bias potential V_{G_B} is provided to the gates of each of transistors 602, 604, 606, and 608 via terminal 622 and resistor 620 (transistors 602 and 606 only). An input signal V_{edin} is provided to self-mixer 600 at terminal 624 and an output signal V_{edo} is sensed from self-mixer 600 at terminal 626.

[0054] In accordance with some embodiments, transistors 602, 604, 606, and 608 of self-mixer 600 form a cascade of transistors each operating in one of two different configurations. More particularly, in some embodiments: transistors 604 and 608 operate in a first configuration in which an RF signal V_{edin} is AC coupled at the drains of the transistors; and transistors 602 and 606 operate in a second configuration in which the RF signal V_{edin} is AC coupled at the sources and the gates of the transistors 602 and 606.

[0055] When transistors 604 and 608 are operating in the first configuration, they operate as shown in FIG. 6B in some embodiments. More particularly, in some embodiments, assuming a baseband drain-to-source potential generated as V_{edo} : $V_{gb} = V_{G_B}$; $V_{sb} = 0$; and $V_{db} = V_{edin} + V_{edo}$, and assuming coupling capacitor Cc is open at baseband, equating the baseband current to zero gives:

$$V_{edo} = \frac{(V_{edin})^2}{2V_t} = k_{ed1}(V_{edin})^2$$

[0056] When transistors 602 and 606 are operating in the second configuration, they operate as shown in FIG. 6C in some embodiments. More particularly, in some embodiments, assuming a baseband drain-to-source potential generated as V_{edo} : $V_{gb} = V_{G_B} + V_{edin}$; $V_{sb} = V_{edin} - V_{edo}$; and $V_{db} = 0$, and assuming coupling capacitor C_c is open at baseband, equating the baseband current to zero gives:

$$V_{edo,1t} = \frac{(2-n)(V_{edin})^2}{2nV_t} = k_{ed1}(V_{edin})^2$$

[0057] When the transistors in these two configurations are cascaded to form a multistage self-mixer as shown in FIG. 6A, on average, the output of each stage at baseband can be written as:

$$V_{edo} = \frac{v_{edin}^2}{2nV_t}$$

[0058] FIGS. 7A and 7B show examples of small-signal models at RF and baseband frequency, respectively, of the circuit in FIG. 6A, in accordance with some embodiments.

[0059] As shown in FIG. 7A, multiple stages appear in parallel at RF, thus the input resistance of the 4-stage self-mixer of FIG. 6A at RF is $4r_o/4$ or r_o .

[0060] As shown in FIG. 7B, the model does not have multi-stage closed loops at baseband, therefore the loading is capacitive. For N -stages the baseband output is:

$$v_{edo} = k_{ed}v_{edin}^2 = N \frac{(v_{edin})^2}{2nV_t}$$

where the conversion constant k_{ed} is $N/(2nV_t)$. Multiple stages appear in series at baseband, thus the output resistance is $N \cdot r_o$; therefore $R_{out,ed}$ equals $N^2 R_{in,ed}$. The output noise PSD in the signal bandwidth of interest is then $PSD_{vn,ed}$ equals $4k_B T N^2 R_{in,ed}$.

[0061] Turning to FIG. 8, an example 800 of a one-transistor, differential self-mixer in accordance with some embodiments is shown. As illustrated, self-mixer 800 includes NMOS FET T1 802, coupling capacitors C_C 804 and 806, and bias resistor R1 808.

[0062] In some embodiments, during operation of one-transistor, differential self-mixer 800: the drain of T1 is grounded; the coupling capacitors C_C are assumed to act as shorts at RF and opens at baseband; the source is floating (so the source has the same DC potential as the drain); the DC bias at the gate of T1 is V_{G_BN} ; and RF signals $V_{rf} = V_{edin}/2$ and $-V_{rf} = -V_{edin}/2$ are AC coupled to the gate and the source of T1, respectively.

[0063] Assuming that the baseband signal generated across drain and source due to second-order non-linearity is small, $V_{gb} = V_{G_B} + V_{rf}$, $V_{sb} = V_{edo,1t} - V_{rf}$, and $V_{db} = 0$ in some embodiments. For small V_{rf} , using the Taylor series expansion and neglecting higher order terms:

$$I_{ds} = K \left(\frac{v_{rf} - V_{edo,1t}}{V_t} \right) + K \left(\frac{v_{rf}}{V_t} \right)^2 \left[\frac{2+n}{2n} \right]$$

where:

$$K = I_s (W/L) e^{V_{G_BN}/(nV_t)},$$

[0064] This leads to the equivalent small-signal model at baseband shown in FIG. 9. The first term is proportional to the drain-to-source potential $V_{db} - V_{sb}$ and can be represented as a resistor r_o as follows:

$$r_o = \frac{V_t}{K} = \frac{V_t}{I_s} \frac{L}{W} e^{-V_{G_BN}/(nV_t)}$$

The second term can be represented as an i_{ds} current source:

$$V_{edo,1t} = i_{ds}r_o = \left[\frac{2+n}{2n} \right] \frac{(v_{rf})^2}{V_t} = k_{edn}(v_{rf})^2$$

[0065] FIG. 10 shows an example 1000 of a complete stage of a differential self-mixer combining a PMOS transistor pair (T3, T4) and an NMOS transistor pair (T1, T2) in accordance with some embodiments. A common-mode voltage V_{CM} is provided at the drains of T3 and T4. The corresponding gate bias voltage for PMOS transistors T3 and T4 is V_{G_BP} . In the presence of an RF signal, a drain-to-source potential is generated across all transistors. Because the current polarities for PMOS transistors and NMOS transistors are opposite, the voltages across T3 and T1 get added and the observed output potential across 1-stage at baseband can be written as:

$$v_{out} = k_{ed}v_{edin}^2 = N \left[\frac{2+n}{4n} \right] \frac{(v_{edin})^2}{V_t}$$

[0066] FIG. 11 illustrates an example of a small-signal equivalent model of the circuit in FIG. 10 in accordance with some embodiments.

[0067] The self-mixer stages of FIG. 10 can be cascaded into a differential multi-stage self-mixer, in some embodiments. For example, in some embodiments, a differential multi-stage self-mixer can be implemented as shown in FIG. 12.

[0068] In some embodiments, the cascading stages in FIG. 12 are configured to not form any closed loops, hence the load created by the stages is capacitive. A common-mode potential V_{CM} can be provided at the drain of the middle stage in FIG. 12 in some embodiments. For N -stages, the conversion equation for self-mixer can be represented as follows in some embodiments:

$$v_{out} = k_{ed}v_{edin}^2 = N \left[\frac{2+n}{4n} \right] \frac{(v_{edin})^2}{V_t}$$

and the conversion constant k_{ed} for the N -stage self-mixer can be represented as follows in some embodiments: $N(2+n)/4nV_t$.

[0069] The N stages appear in parallel at RF and in series at baseband in some embodiments. Hence, the differential input resistance at RF is $R_{in} = r_o/N$, while the differential output resistance at baseband is $R_{out} = Nr_o$, and thus $R_{out} = N^2R_{in}$. The output noise variance of the self-mixer is then:

$$\sigma_{vn,ed}^2 = 4K_B T N^2 R_{in} BW_{BB}$$

wherein K_B is the Boltzmann constant and BW_{BB} is the baseband bandwidth of the input signal.

[0070] As shown in FIG. 13, in accordance with some embodiments, the bias potentials V_{G_BN} and V_{G_BP} for biasing the self-mixer transistors T1, T2, T3 and T4 can be generated by comparing a replica of these transistors with a 10 M Ω poly-resistor (illustrated in FIG. 13 as two 5 M Ω resistors) used in a 2 nA PTAT (proportional to absolute temperature) current reference circuit. This PTAT current reference circuit biases transistors T9 and T10 to set the desired resistance. The generated DC potentials V_{G_BN} and V_{G_BP} for NMOS and PMOS, respectively, set the resistance of T1, T2, T3, and T4. This current-controlled biasing technique makes the self-mixer resilient to process and temperature variations.

[0071] The signal-to-noise ratio at the output of the self-mixer is:

$$SNR_{edo} = \frac{1}{4K_B T BW_{BB}} \left[\frac{2+n}{4n} \right]^2 \frac{A_v^4 P_{in}^2 R_s^2}{R_{in} V_t^2}$$

[0072] Both signal power and noise power increases in proportion to N^2 . Thus, the SNR is independent of the number of stages used. Therefore, an increased number of stages does not

improve sensitivity. However, it does provide an additional baseband gain which helps in reducing the power consumption of the baseband circuits.

[0073] The output signal is proportional to N , therefore, multiple stages can be treated as providing passive gain before the baseband in some embodiments. This passive gain relaxes the noise requirements and reduces the active power consumption of the baseband circuits in some embodiments.

[0074] With increasing number of self-mixer stages, the provided bandwidth decreases. The self-mixer can be treated as an RC transmission line, where the resistance $R_{tx} = R_{in,ed}N$ and the capacitance $C_{tx} = C_C$. The step input to output transfer function for a transmission line with an open circuit load is the error function:

$$v_{cds}(t) = v_{cds} \operatorname{erf} \left(\frac{N \sqrt{R_{tx} C_{tx}}}{2\sqrt{t}} \right)$$

[0075] Thus, the equivalent bandwidth is $0.46/(N^2 R_{tx} C_{tx})$. With increasing number of stages, the available baseband bandwidth reduces.

[0076] Turning to FIG. 14, an example 1400 of a wake-up receiver architecture in accordance with some embodiments is shown. As illustrated, architecture 1400 includes an antenna 1402, a matching network 1404, a 40-stage self-mixer 1406, a current-reuse inverter-based voltage amplifier 1408, a matched filter 1412, a comparator 1414, a correlator 1416, a clock source 1418, and a digital control circuit 1420.

[0077] In some embodiments, architecture 1400 is configured to detect an 11-bit wake-up code that is on-off-key (OOK) modulated at data-rate f_{DATA} of 100 bps on an RF carrier.

[0078] In architecture 1400, time-encoded clocked integration using clock-triggered voltage-controlled delay lines (VCDL) can be used to implement a matched filter for the rectangular-bit

shape to reduce baseband noise. The outputs of the VCDLs can then be compared using a phase-frequency detector (PFD). PFD UP/DOWN output pulses from the PFD can then drive a Set-Reset latch in comparator 1414. This effectively implements a comparator or a 1-bit ADC for the time-encoded signal. The comparator can be clocked at a sampling rate $f_S = 2 f_{\text{DATA}}$ to effect 2x oversampling. The PFD output pulses can also be fed back to the self-mixer reference node via a charge pump in 1410. This creates a first order, low bandwidth, delay-locked loop to reject DC signals due to any DC offsets introduced by the baseband signal processing circuits or due to a continuous-wave interferer at the receiver input (as described below in connection with FIGS. 19 and 20).

[0079] To better understand how a self-mixer's design impacts a receiver front end that incorporates the self-mixer, assume that a received RF input signal, $V_{in}(t)$, is an amplitude modulated signal at a carrier frequency f_{RF} and is incident on an antenna of the receiver with a radiation resistance R_S . The root-mean squared (RMS) voltage signal at the antenna is $V_{in,RMS}^2 = P_{in}R_S$ wherein P_{in} is the received signal power. An L-C matching network of the receiver then amplifies this voltage with a passive voltage gain $A_v = V_{edin}/V_{in}$. This A_v depends on the load resistance $R_{in,ed}$ and the capacitance C_{in} of the self-mixer. C_{in} may be a combination of the capacitances from any off-chip inductor (in the matching network), packaging, bond-wire(s), an on-chip electrostatic discharge (ESD) circuit, the self-mixer, and/or any other connected components in some embodiments. Assuming that an inductor with value $L_{ind} \approx 1/(\omega_{\text{RF}}^2 C_{in})$ with a self-resonance frequency much higher than $\omega_{\text{RF}}/(2\pi)$ and a quality factor Q_{ind} is used in the matching network, an optimal $R_{in,ed}$ may be $R_{in,ed} = Q_{ind}/(\omega_{\text{RF}} C_{in})$ in some embodiments. For example, in some embodiments, for a Q_{ind} of 80 and a capacitance C_{in} of 1pF at 434 MHz, an

optimal $R_{in,ed}$ for the self-mixer may be $30k\Omega$. The passive gain from the matching network may then be $A_v = \sqrt{R_{in,ed}/(2R_s)}$ in some embodiments.

[0080] In accordance with some embodiments, the conversion gain constant k_{ed} of a self-mixer can be $N/(2nV_t)$, and the output noise PSD of a self-mixer can be written as $PSD_{vn,edo} = 4k_B T N^2 R_{in,ed}$.

[0081] In some embodiments, the receiver sensitivity for a continuous-wave RF input signal as a function of self-mixer $R_{in,ed}$, matching network A_v , baseband noise-figure NF, required SNR_{req} and baseband sampling rate f_s can be:

$$Sensitivity_{\text{dBm}} = \frac{1}{2} (SNR_{req, \text{dB}} + NF_{\text{dB}}) - A_v_{\text{dB}} + 10 \log \left[\sqrt{\frac{4k_B T R_{in,ed} f_s (2nV_t)^2}{R_s^2}} / \text{Im}W \right]$$

[0082] FIG. 15 shows an example implementation of a self-mixer and a baseband amplifier in accordance with some embodiments. Although specific size components and types of components are described in connection with FIG. 15, it should be apparent that other suitable size components and types of components can be used in some embodiments.

[0083] As illustrated in FIG. 15, the source of the self-mixer, V_{EDREF} , is floating and connected to a 20pF capacitor that is driven by a charge pump; this creates a DC feedback loop. The output of the self-mixer, $V_{ed,bbo}$, is connected to the baseband-amplifier NMOS transistor M_{A1} . The self-mixer operates in the linear region, and the DC gate potential of M_{A1} is the same as DC potential at V_{EDREF} .

[0084] The DC gate bias V_{G_B} of the self-mixer leads to a gate-to-drain leakage current. If uncompensated, this current could increase the potential V_{EDREF} , negating the effect of gate-biasing. FIG. 15 shows a leakage-compensation circuit in which a replica self-mixer (without C_c

and C_L) is used to sense the leakage current using transistor M_{L1} ; this current is mirrored to M_{L2} and compensates for the leakage in the self-mixer. A varying V_{EDREF} can change the leakage current. In order to address this, an operational amplifier in the leakage-compensation circuit controls the current mirror using a replica self-mixer circuit to compensate for the leakage so that the DC potential at V_{EDREF} is fixed.

[0085] FIG. 15 also shows a biasing circuit that can be used to generate V_{G_B} and V_{RES_BIAS} in some embodiments. As shown, the biasing circuit includes a replica M_{A2} of the NMOS transistor M_{A1} . The biasing circuit also includes a series of 40 self-mixer replica transistors, wherein each of the 40 replica transistors is the same size as a corresponding transistor in the 40-stage self-mixer to keep track of the threshold variations. This is operated as a source follower with a drain current source of I_{BIAS_RECT} . The current source I_{BIAS_AMP} sets the gate-to-source potential for M_{A2} . The current source I_{BIAS_RECT} sets the potential V_{G_B} . This current-controlled biasing technique makes the self-mixer resilient to voltage and process variations.

[0086] Transistor M_{R2} is biased as a resistor for AC-coupling the RF signal in the self-mixer. A replica transistor M_{R3} is used to generate the bias potential V_{RES_BIAS} for setting the resistance of M_{R2} .

[0087] FIG. 16 shows a more detailed schematic of a wake-up receiver in accordance with some embodiments. Although specific size components and types of components are described in connection with FIG. 16, it should be apparent that other suitable size components and types of components can be used in some embodiments.

[0088] In some embodiments, the receiver shown in FIG. 16 can be implemented to operate at any suitable frequency. For example, in some embodiments, receiver(s) can be implemented

to operate at 151.25 MHz, 434.4 MHz and/or 1.016 GHz using the matching network design in FIG. 16 with the component values below:

Frequency	L_{ind}	Inductor Details	C_1
151.25 MHz	1 μ H	26 AWG Cu 13 turns	30pF
434.4 MHz	111 nH	132-10SM Coilcraft	14pF
1.016 GHz	27 nH	0908-SQ Coilcraft	3.3 nH*

*Note: The Q-factor of the capacitors degrades with increasing frequency. Thus, for the 1.016 GHz implementation, a matching network with 3.3 nH inductor can be used instead of capacitor C_1 to reduce losses.

[0089] As shown in FIG. 16, the output of the matching network is connected to the 40-stage self-mixer with an $R_{in,ed}$ of 200 k Ω at 151 MHz and 434.4 MHz and 50 k Ω at 1.016 GHz. The source of the multi-stage self-mixer $V_{edref} = V_{EDREF} + v_{edref}(t)$ is connected to a delay-locked loop (DLL).

[0090] The self-mixer output, $v_{ed,bb0}$, is amplified by gain ($-A_{v,amp}$) of 26 dB using a current-reuse baseband amplifier with output $v_{o,amp}(t)$. Its input-referred noise is $2kTn/(g_m)$; assuming $n = 1.2$ and $g_m/I_d = 29$, an $I_d = 370$ pA, the amplifier NF compared to the self-mixer output noise ($R_{in,ed} = 200$ k Ω) is 1 dB while the power consumption is only 150 pW at 0.4 V. The PMOS transistor is current biased using a current mirror with AC coupling while the NMOS transistor is biased through the DC feedback loop created by the DLL. Additionally, the DLL provides a high-pass response in the signal path and rejects the low-frequency flicker noise added by the amplifier.

[0091] A windowed integrator implementation using time-encoded analog signals can be adapted to be used as a matched detector for the rectangular bit shape; it filters the high-

frequency baseband noise and ensures that the noise bandwidth is f_s to optimize the SNR before sampling.

[0092] Two voltage-controlled delay lines (VCDLA and VCDLB) (FIG. 16) with clocked feedback realize a V-to-T signal conversion and time-encoded integration. The operation principle is illustrated in FIG. 18. The rising-edge of the OSC_CLK triggers oscillation in VCDLs, with the frequency controlled by its respective input voltage, $V_{o,amp}$ and $V_{DELAY,REF}$. At the falling-edge of OSC_CLK, the relative position of the edges in VCDLs has the information of the output phase (relative delay), effectively integrating the input signal when OSC_CLK is "high." For an OSC_CLK time period T_p , the VCDLs integrate the signal for a time of $7T_p/8$ and remain in reset mode for the rest of the period. This is ensured by deriving the OSC_CLK from an 8x REF_CLK generated using an on-chip current-starved ring oscillator. Assuming the DC output of the amplifier is set as $V_{DELAY,REF}$ using the DC feedback for the DLL, the difference of the output pulse widths of the two VCDLs is:

$$\Delta t_l[kT_p] = \int_{(k-7/8)T_p}^{kT_p} K_{vco} T_{vco} v_{o,amp}(t) dt$$

where K_{vco} is the voltage-to-frequency conversion gain and $T_{vco} = 1/f_{vco}$ is the time period when VCDLA is operated as a VCO, and k is the index for the discrete-time samples. In z-domain:

$$\Delta t_l(z) = \frac{-7}{8} A_{v,amp} K_{vco} T_{vco} T_p \frac{V_{edref}(z)}{z} + sig(z)$$

where $sig(z)$ is the Z-transform of the discrete samples $sig[kT_p]$:

$$sig[kT_p] = -A_{v,amp} K_{vco} T_{vco} \int_{(k-7/8)T_p}^{kT_p} v_{edo}(t) dt$$

[0093] This can be used to evaluate the time-domain response of the DLL.

[0094] At the end of the OSC_CLK "high" pulse, Δt_l is measured using phase-frequency detector (PFD). The relative pulse-widths of the UP/DOWN pulses provides a measure if $\Delta t_l \geq 0 | \Delta t_l \leq 0$. These UP/DOWN pulses trigger an SR-latch to operate as a comparator. The output of the SR-latch is sent to an 11-bit digital correlator.

[0095] A non-zero threshold for the comparator needs to be set for a low false-alarm rate. The DLL sets $\Delta t_l = 0$ at the output of the VCDLs. Additional current-starved inverter delay cells in the signal and reference path with a different delay (τ_N and τ_P) are added in each branch after VCDLs to set the threshold. The threshold can be configured for false alarm to be less than one per hour in some embodiments.

[0096] The receiver uses 2x oversampling to receive the wake-up code. As a result, either the even or the odd samples will be aligned with the incoming data signal. The on-chip 100 pW 11-bit sliding-window digital correlator skips every alternate bit and thus correlates with the most reliable data. D-flipflop shift registers keep the last twenty-two samples, XOR gates multiply the received code with the desired wake-up code, and a 4-bit full-adder sums the XOR outputs; the adder output is then compared with a correlation threshold.

[0097] $\Delta t_l[kT_p]$ is also sensed using a separate PFD and is fed back to the reference input of the self-mixer using a charge pump with a load capacitor C_{lf} as shown in FIG. 16. The loop sets $\Delta t_l = 0$ at DC, thus forming a delay-locked loop. This sets the amplifier output DC potential equal to V_{EDREF} , which then biases the voltage amplifier as well.

[0098] The charge-pump output can be written as $v_{\text{edref}}[kT_p] = v_{\text{edref}}((k-1)T_p) + I_{\text{CP}}\Delta t_l(kT_p)/C_{\text{lf}}$, where I_{CP} is the charge-pump current of 1 pA and C_{lf} is a load capacitor of 20 pF. This feedback loop is enabled for every alternate sample for a time of $T_p/8$ at the end of integration cycle controlled by CP_EN in FIG. 17. The discrete-time operation of the DLL justifies the use of a Z-domain model for analysis as shown in FIG. 18. The Z-domain transfer function from $\text{sig}(z)$ to $\Delta t_l(z)$ is:

$$\frac{\Delta t_l(z)}{\text{sig}(z)} = \frac{1 - z^{-1}}{1 - (1 - G_{\text{loop}})z^{-1}}$$

where loop gain: $G_{\text{loop}} = (7T_p/8)A_{\text{v,amp}}K_{\text{vco}}T_{\text{vco}}I_{\text{CP}}/C_{\text{lf}}$. The transfer function represents a high pass filter with a cutoff frequency of $f_s/100$, with $f_s=200$ Hz.

[0099] In some embodiments, the settling time of the DLL may limit the number of consecutive "1"s in the wake-up code to three (or any other suitable value). If a code with more consecutive "1"s is necessary or desirable, RZ-encoding or Manchester encoding can be used in some embodiments.

[0100] The region of convergence (ROC) is defined by $|z| > |(1 - G_{\text{loop}})|$. For a causal and stable linear time invariant system, the ROC must extend the outermost pole to infinity and must include the unit circle $|z| = 1$ in some embodiments. Therefore, G_{loop} must be less than 1 in some embodiments. This sets the charge-pump current I_{CP} and capacitance C_{lf} .

[0101] The amplifier and the VCDLs add random DC offsets modeled as $V_{\text{OFF,AMP}}$ and $V_{\text{OFF,OSC}}$ in FIG. 18. The charge pump in the feedback loop creates a zero at DC, so that the DC offsets are rejected. Thanks to this baseband offset cancellation, very small transistors can be used in the VCDLs, even though they introduce larger mismatches, and the VCDLs can operate with only 50 pW each.

[0102] The comparator threshold can be set sufficiently large so that there is a low probability to trigger a false wake-up at any suitable rate (e.g., less than one per hour).

[0103] The false-alarm probability is the probability that the comparator output is the desired wake-up code due to the noise present in the receiver. Assuming a receiver sampling rate of f_s , the total number of bits received in an hour is $3600 \cdot f_s$. Let H be the number of "1"s in a wake-up code. For x -bit error tolerance in the correlator, the total number of false positives generated are approximately equal to $3600 f_s^H C_x P^{H-x}$ where P is the probability of comparator output to be "1". It is assumed that the probability of receiving a "0" is close to 1 for simplicity.

Therefore, P is required to be less than:

$$\left(1 / \left((3600 f_s^H C_x)^{1/(H-x)} \right)\right)$$

for a false alarm rate of less than one per hour. For f_s equal to 200 samples per second and a desired 11-bit wake-up code "11100100110" received with 1-bit error tolerance, the required P can be 4.7%. Assuming a Gaussian noise distribution, the corresponding threshold required is

$$\tau_d = 1.7\sigma = 1.7 \sqrt{\Delta t_{j,ed}^2}, \text{ wherein } \Delta t_{j,ed}^2 \text{ is the jitter contribution due to the self-mixer.}$$

[0104] In some embodiments, at least a certain SNR may be required at the input of the comparator for successful detection of a wake-up code based on the comparator threshold derived above for a given false-alarm rate. For an x -bit error tolerance, the receiver must miss at least $(x + 1)$ bits in order to miss a wake-up signal. Assuming that the probability of missing $(x + 2)$ bits or more in a code will be low compared to missing only $(x + 1)$ bits, the probability of missed detection is approximately equal to ${}^H C_{x+1} P_1^{x+1}$, where P_1 is the probability of a missed bit. For a required missed-detection ratio (MDR) of 10^{-3} , with $N = 6$, and 1-bit error tolerance, P_1 is required to be 0.008, requiring the input signal of the comparator to be 2.4σ above the

threshold. Therefore, a total signal amplitude of 4.1σ is required for signal detection, thus requiring a 12.3 dB SNR at the input of the comparator.

[0105] In some embodiments, a receiver can be implemented to account for one or more interferers received at the receiver's antenna.

[0106] For example, in some embodiments, as shown in FIG. 19, a receiver 1900 having a low frequency path and a high frequency path can be used to account for an interferer. As illustrated, receiver 1900 includes an antenna 1902, a four-element passive balun 1904, a matching network 1906, a differential self-mixer 1908, a low frequency (LF) path 1910, a high frequency (HF) path 1912, a low-pass filter and hysteresis comparator 1914, a high-pass filter and hysteresis comparator 1916, a clock 1918, an envelope detector 1920, sliding window correlators 1926 and 1928, and an adder 1930. It should be noted that some inductor and capacitor values are shown for illustrative purposes in FIG. 19 and that other values can be used in some embodiments.

[0107] In some embodiments, any suitable type of interferer can be accounted for.

[0108] For example, in accordance with some embodiments, assume that an interferer V_{int} that is a constant amplitude sine wave (i.e., with no amplitude or phase modulation) is received. FIG. 20 shows an example of corresponding spectra at the input and output of differential self-mixer 1908 of receiver 1900 of FIG. 19 that may be seen for this interferer. In the differential self-mixer, V_{int} 2002 acts as a local oscillator (LO) and mixes with a wanted signal V_{wanted} 2004 to generate a copy of the desired signal at the IF frequency as $V_{mix,if}$ 2006 while $V_{int,bb}$ 2008 is a signal at DC, typically larger than $V_{sig,bb}$ 2010. These signals may then be processed in the low frequency (LF) and high frequency (HF) paths.

[0109] In the LF path, the baseband signal is amplified (by self-mixer 1908), low-pass filtered (by the low-pass filter of 1914 so that the filter attenuates high-frequency signals (in this case, $V_{\text{mix,if}}$ 2016 of FIG. 20), and passes low-frequency signals (in this case, $V_{\text{sig,bb}}$ 2018 of FIG. 20)) and then sliced (by the hysteresis comparator of 1914) to remove the high-frequency signals.

[0110] In the HF path, the baseband signal is amplified (by self-mixer 1908), high-pass filtered (by the high-pass filter of 1916 so that the filter attenuates low-frequency signals (in this case, $V_{\text{sig,bb}}$ 2029), and passes high-frequency signals (in this case, $V_{\text{mix,if}}$ 2022)), and sliced (by the hysteresis comparator of 1916) to remove the low-frequency signals, and then envelope detection is performed (by envelope detector 1920) to demodulate the signal.

[0111] In some embodiments, signal $V_{\text{mix,if}}$ in the HF path can increase one dB per one dB increase in interferer power while noise from the self-mixer remains constant. Thus, the sensitivity of the receiver in the HF path can improve by one dB for one dB increase in the interferer power in some embodiments.

[0112] As another example of a type of interferer that can be accounted for in some embodiments, assume that a strong phase modulated (PM) or frequency modulated (FM) interferer (i.e., with no amplitude modulation, but with phase modulation) is received. In this case, $V_{\text{sig,bb}}$ and $V_{\text{int,bb}}$ are independent of the phase modulation. Also, in this case, $V_{\text{mix,if}}$ carries the amplitude modulation of the wanted signal and the phase modulation of the interferer. Therefore, $V_{\text{mix,if}}$ can be demodulated using the envelope detector in the HF path, to make it insensitive to the phase modulation of the interferer. Hence, the receiver can treat a PM/FM interferer as a narrowband carrier and have the performance as described above for the signal in the presence of a narrowband carrier.

[0113] As yet another example of a type of interferer that can be accounted for in some embodiments, assume that an AM interferer is received. FIG. 21 shows an example of corresponding spectra at the input and output of differential self-mixer 1908 of receiver 1900 of FIG. 19 that may be seen for this interferer. As shown in area 2102, the frequency content of the interferer $V_{\text{int,bb}}$ may overlap with the content of the wanted signal $V_{\text{sig,bb}}$ and for a strong AM interferer the wanted signal in the LF-path may get blocked by the strong AM interferer as shown by signal 2014.

[0114] However, in some embodiments, $V_{\text{mix,if}}$ can be processed in the HF-path to obtain the wanted signal. The modulation of the wanted signal is a random stream of "1"s and "0"s as shown by the middle waveform of FIG. 22. For an AM interferer with low-modulation index (e.g., $m_{\text{int}}(t) \ll 1$), $V_{\text{mix,if}}$ will have an IF frequency ($\omega_{\text{sig}} - \omega_{\text{int}}$) output in the presence of "1", and no signal in the presence of "0" as shown by the bottom waveform in FIG. 22. This signal is then amplified with a limiting amplifier to remove the unwanted AM modulation of $m_{\text{int}}(t)$ and the wanted signal is retrieved using envelope detection at the IF frequency.

[0115] Referring back to FIG. 19, more details are now provided regarding the operation of receiver 1900. While specific values of components are provided herein for purposes of illustration, it should be understood that any other suitable values of components can be used in some embodiments.

[0116] As shown in FIG. 19, the receiver front end first converts a 50Ω antenna impedance into a 100Ω differential impedance using four-element passive balun 1904 that include inductors L1 (which can each have a value of 20 nH or any other suitable value(s) in some embodiments) and capacitors C1 (which can each have a value of 4 pF or any other suitable value(s) in some embodiments). The 100Ω differential impedance is then matched to the self-mixer's input

resistance (which can have a value of 25 k Ω or any other suitable value in some embodiments) using a three-element matching network that includes a capacitor C2 (which can have a value of 5.6 pF or any other suitable value in some embodiments) and inductors L2 (which can each have a value of 100 nH or any other suitable value(s) in some embodiments, and which can each have a Q-factor of 30 (or any other suitable value(s)) at 550 MHz (or any other suitable value(s)) in some embodiments). A passive voltage gain may then be realized in some embodiments.

[0117] Next, RF-to-baseband down-conversion can be implemented by components 1908, 1914, and 1916. In some embodiments, these components can be implemented in any suitable manner. For example, in some embodiments, components 1908, 1914, and 1916 can be implemented using example architecture 2300 shown in FIG. 23.

[0118] Architecture 2300 can include differential input capacitances at input terminals 2302 that can include any suitable capacitances at the RF input of the packaged chip including package (including bond-wire) capacitances, ESD capacitances, and self-mixer capacitances, which can be 165 fF, 65 fF and 188 fF, respectively, or any other suitable values in some embodiments.

[0119] In some embodiments, two-bit on-chip trim capacitors 2304 can be included to fine tune the matching network to the desired RF frequency. As illustrated in FIG. 23, by setting the switch in 2304, the capacitances at terminals 2302 can be adjusted.

[0120] A 10-stage self-mixer 2306 can be connected to terminals 2302.

[0121] Architecture may further include an LF path 2308 and an HF path 2310, that can operate in an identical or similar manner to the LF path and the HF path described above. Path 2308 can include a baseband low-noise amplifier (BB_LNA_LF) 2312, a baseband amplifier (BB_AMP_LF) 2314, a low-pass filter (LPF) 2316, a baseband variable-gain amplifier

(BB_VGA_LF) 2318, and a hysteresis comparator 2320. Path 2310 can include a baseband low-noise amplifier (BB_LNA_HF) 2322, a high-pass filter (HPF) 2324, a baseband amplifier (BB_AMP_HF) 2326, a baseband variable gain amplifier (BB_VGA_HF) 2328, and a hysteresis comparator 2330.

[0122] In some embodiments, the outputs of the LF and HF paths can be correlated off-chip with a Barker-code using sliding-window correlators 1926 and 1928 of FIG. 19.

[0123] During regular operation of the receiver, the LF-path demodulates the signal with a baseband LNA and a low-pass filter that filters inter-modulation products at the self-mixer output.

[0124] As shown in FIG. 24, BB_LNA_LF 2312, BB_AMP_LF 2314, BB_VGA_LF 2318, BB_LNA_HF 2322, BB_AMP_HF 2326, and BB_VGA_HF 2328 can be implemented as common-source differential amplifiers in some embodiments. The table in the figures gives example values for the different components of the figure depending on the application in FIG. 23.

[0125] When the circuit in FIG. 24 is used to implement an LNA (e.g., BB_LNA_LF 2312 or BB_LNA_HF 2322), body biasing techniques can be used to control the V_{TH} variations of NMOS transistors T1, T2, T5, and T6, allowing the operation of the LNA at 0.5 V (or any other suitable voltage). The LNA can be AC-coupled to the self-mixer using PMOS transistors (T3, T4) operating in the linear region as 250 M Ω resistors and providing a 10 kHz high-pass cutoff for 400kpbs data rate in some embodiments. Transistors T5 and T6 can be used as resistors for common-mode feedback in some embodiments.

[0126] When the circuit in FIG. 24 is used to implement a VGA, the variable gain can be implemented using 3-bit programmable common-mode feedback resistors implemented with T5 and T6 in some embodiments.

[0127] As shown in FIG. 25, LPF 2316 can be implemented as a third-order, current-biased, g_m -C, 500 kHz, Chebyshev low-pass filter for 400 kbps data rate in some embodiments. In some embodiments, this filter can be used in the LF path to reject the mixer output products beyond 1 MHz. MOS-capacitors can be used for small capacitors C1, C2 and C3. In some embodiments, the transconductors in FIG. 25 can be implemented in the same manner as BB_LNA_LF 2312 in FIG. 24. In some embodiments, the transconductors can operate in weak inversion, causing a PTAT current source to provide a constant transconductance. This can keep the LPF cutoff constant across temperature to the first order in some embodiments.

[0128] As shown in FIG. 26, HPF 2324 can be implemented as a third-order, 1MHz, Chebyshev g_m -C high-pass filter in some embodiments. In some embodiments, this filter can be used in the HF path to reject any down-converted AM interferer in the baseband. MOS-capacitors can be used to implement C4, C5 and C6 with low capacitance values in some embodiments.

[0129] In some embodiments, Barker codes have correlations very close to a δ function. In some embodiments, the auto-correlation is 11 when the codes are aligned and reduces to $\leq |1|$ at any other bit offset. Hence, the Barker code can be used to help to identify a wanted signal in the presence of an interferer. In some embodiments, the receiver demodulator can use a correlation threshold of 7 to identify the wanted signal.

[0130] In some embodiments, multiple interferers can be accounted for using example architecture 2700 shown in FIG. 27. Architecture 2700 uses multiple IF filters with a 400 kHz

bandwidth located at different IF-frequencies, followed by a correlator-bank to look for the availability of the wanted signal in some embodiments.

[0131] Although the invention has been described and illustrated in the foregoing illustrative embodiments, it is understood that the present disclosure has been made only by way of example, and that numerous changes in the details of embodiment of the invention can be made without departing from the spirit and scope of the invention, which is limited only by the claims that follow. Features of the disclosed embodiments can be combined and rearranged in various ways.

What is claimed is:

1. A circuit for a wake-up receiver comprising:
 - a first self-mixer stage comprising:
 - a first NMOS transistor having a source, a drain, and a gate;
 - a second NMOS transistor having a source, a drain, and a gate, wherein the drain of the second NMOS transistor is connected to the drain of the first NMOS transistor;
 - a first PMOS transistor having a source, a drain, and a gate, wherein the source of the first PMOS transistor is connected to the source of the first NMOS transistor;
 - a second PMOS transistor having a source, a drain, and a gate, wherein the drain of the second PMOS transistor is connected to the drain of the first PMOS transistor, and the source of the second PMOS transistor is connected to the source of the second NMOS transistor;
 - a first resistor having a first side connected to the gate of the first NMOS transistor and having a second side connected to a first gate bias voltage;
 - a second resistor having a first side connected to the gate of the first PMOS transistor and having a second side connected to a second gate bias voltage;
 - a third resistor having a first side connected to the gate of the second NMOS transistor and having a second side connected to the first gate bias voltage;
 - a fourth resistor having a first side connected to the gate of the second PMOS transistor and having a second side connected to the second gate bias voltage;
 - a first coupling capacitor having a first side connected to a first radio frequency (RF) input signal and having a second side connected to the gate of the first NMOS transistor;

a second coupling capacitor having a first side connected to the first RF input signal and having a second side connected to the gate of the first PMOS transistor;

a third coupling capacitor having a first side connected to a second RF input signal and having a second side connected to the gate of the second NMOS transistor;
and

a fourth coupling capacitor having a first side connected to the second RF input signal and having a second side connected to the gate of the second PMOS transistor.

2. The circuit of claim 1, wherein the first self-mixer stage further comprises:

a fifth coupling capacitor having a first side connected to the source of the first NMOS transistor having a second side connected to the second RF input signal; and

a sixth coupling capacitor having a first side connected to the source of the second NMOS transistor and having a second side connected to the first RF input signal.

3. The circuit of claim 1, wherein the drain of the first PMOS transistor is connected to a common mode voltage.

4. The circuit of claim 1, wherein the first RF input signal is an inverted form of the second RF input signal.

5. The circuit of claim 1, further comprising a second self-mixer stage.

6. The circuit of claim 1, further comprising a matching network that provides the first RF input signal and the second RF input signal.
7. The circuit of claim 1, wherein the drain of the first NMOS transistor provides a first output signal and the drain of the first PMOS transistor provides a second output signal.
8. The circuit of claim 7, further comprising a low-pass filter having a first input connected to the first output signal, having a second input connected to the second output signal, having a first output, and having a second output.
9. The circuit of claim 8, further comprising a first hysteresis comparator having a first input connected to the first output of the low pass filter, having a second input connected to the second output of the low pass filter, having a first output, and having a second output.
10. The circuit of claim 9, further comprising a first correlator having a first input connected to the first output of the first hysteresis comparator and having a first output.
11. The circuit of claim 8, further comprising a high pass filter having a first output connected to the first output signal and having a second input connected to the second output signal.

12. The circuit of claim 11, further comprising a second hysteresis comparator having a first input connected to the first output of the high pass filter, having a second input connected to the second output of the high pass filter, having a first output, and having a second output.

13. The circuit of claim 12, further comprising a first envelope detector connected to the first output of the second hysteresis comparator and a second envelope detector connected to the second output of the second hysteresis comparator.

14. The circuit of claim 13, further comprising a second correlator having a first input connected to the first output of the second hysteresis comparator and having a first output.

15. The circuit of claim 14, further comprising an adder connected to the first output of the second correlator.

16. The circuit of claim 14, wherein the second correlator receives a Barker code.

17. The circuit of claim 16, wherein the Barker code is 11 bits.

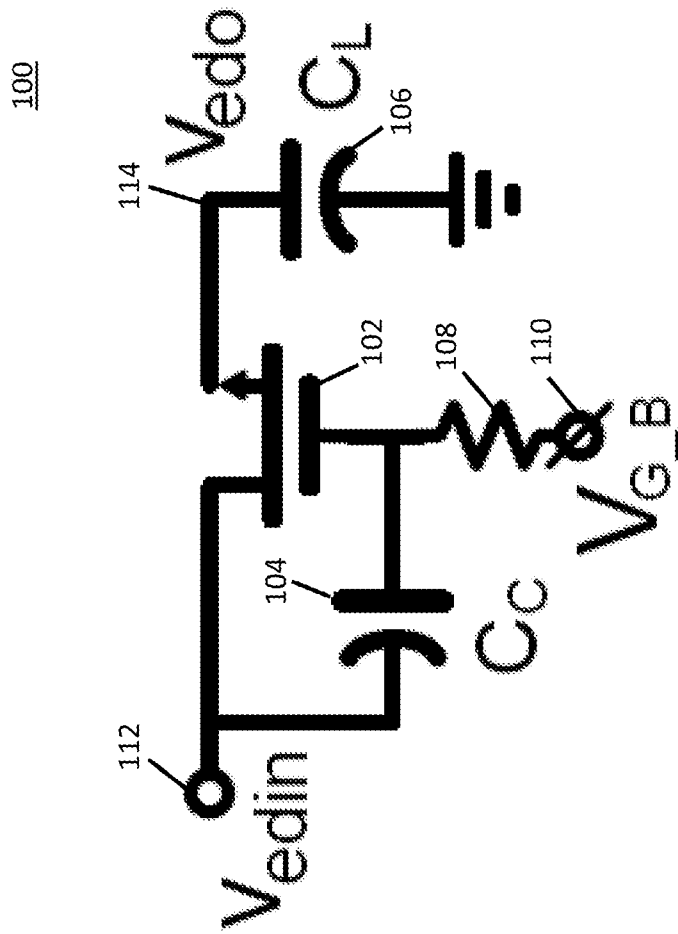


FIG. 1

200

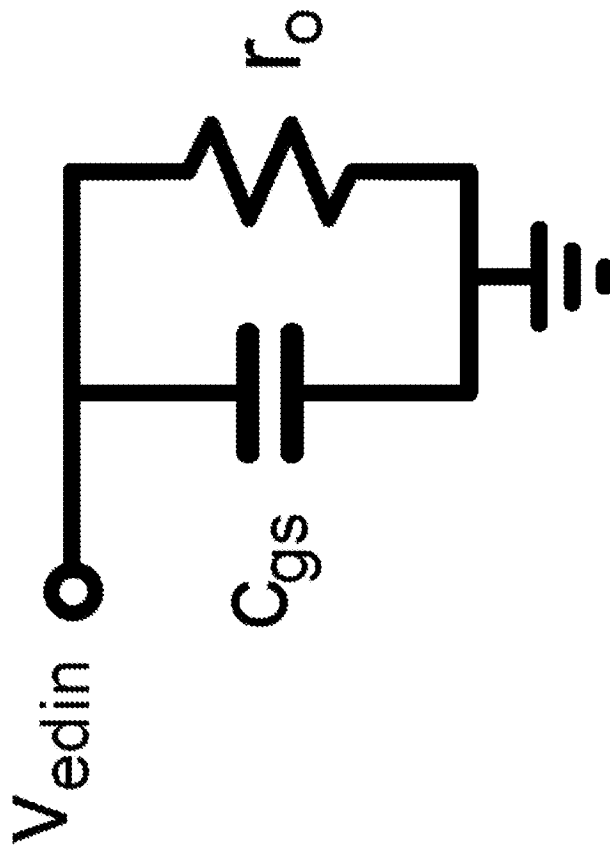


FIG. 2A

250

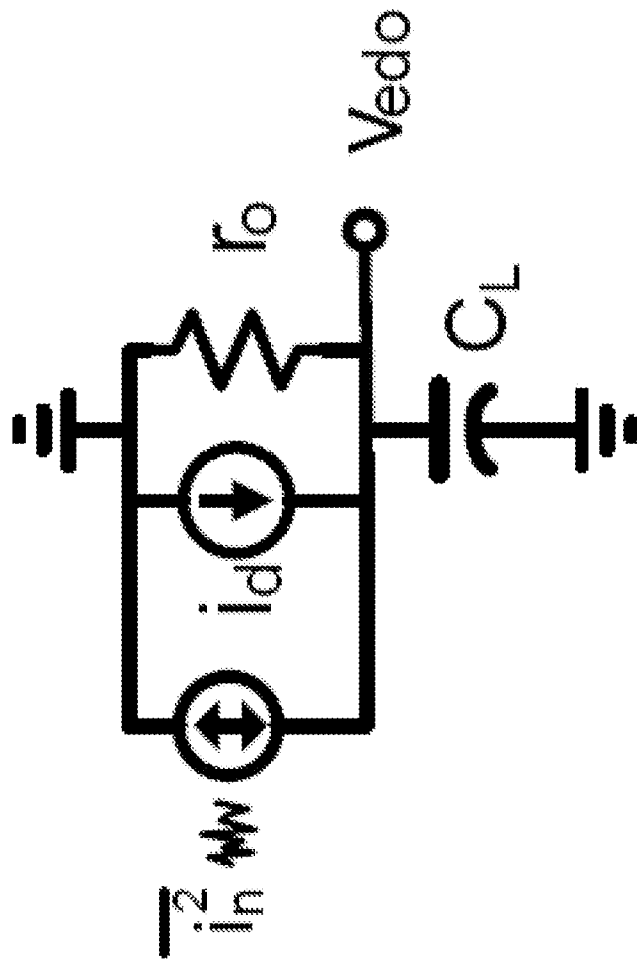


FIG. 2B

300

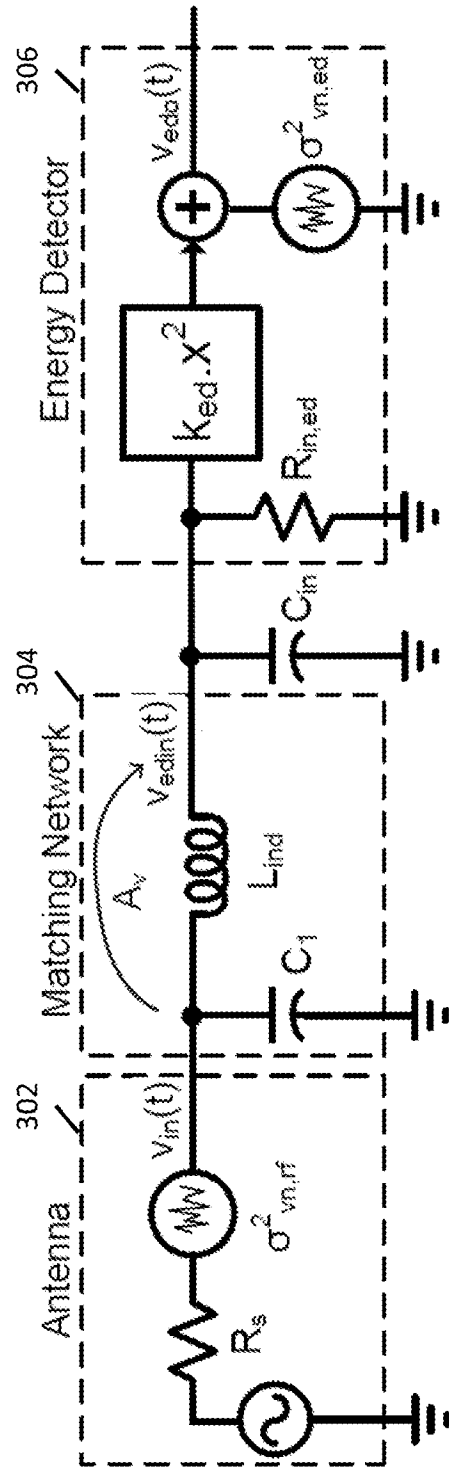


FIG. 3

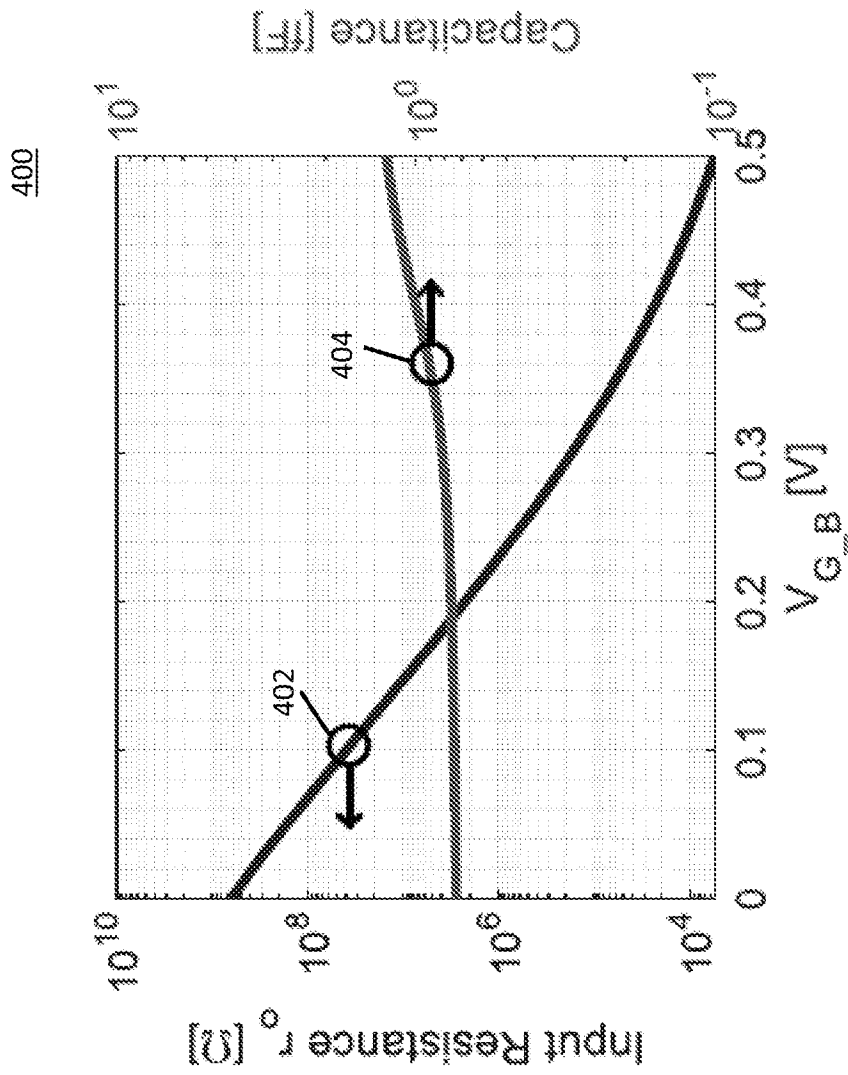


FIG. 4

500

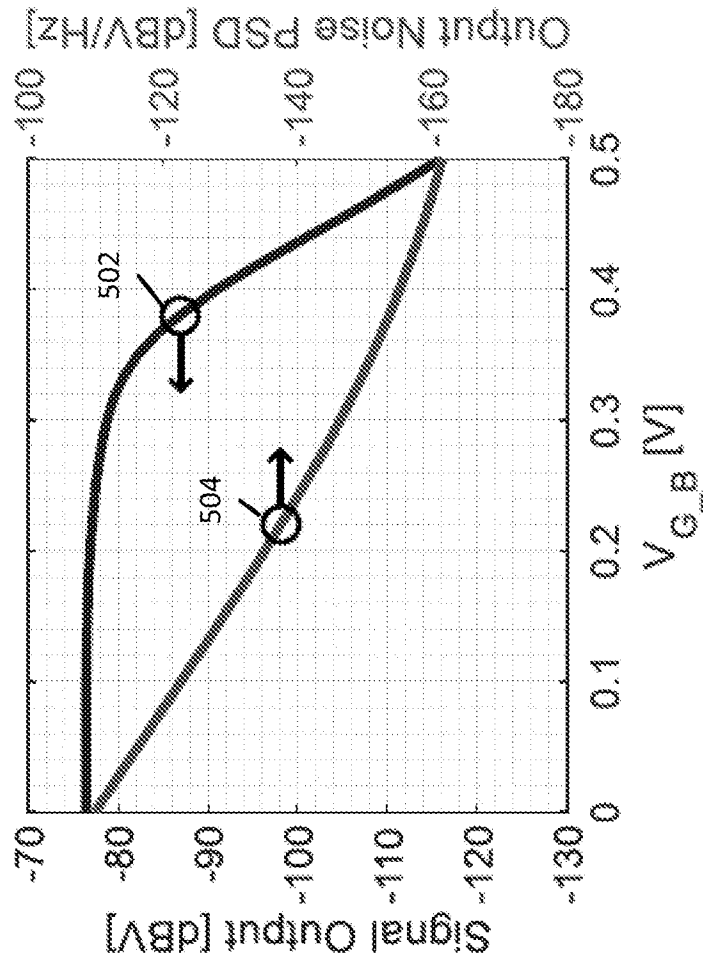


FIG. 5

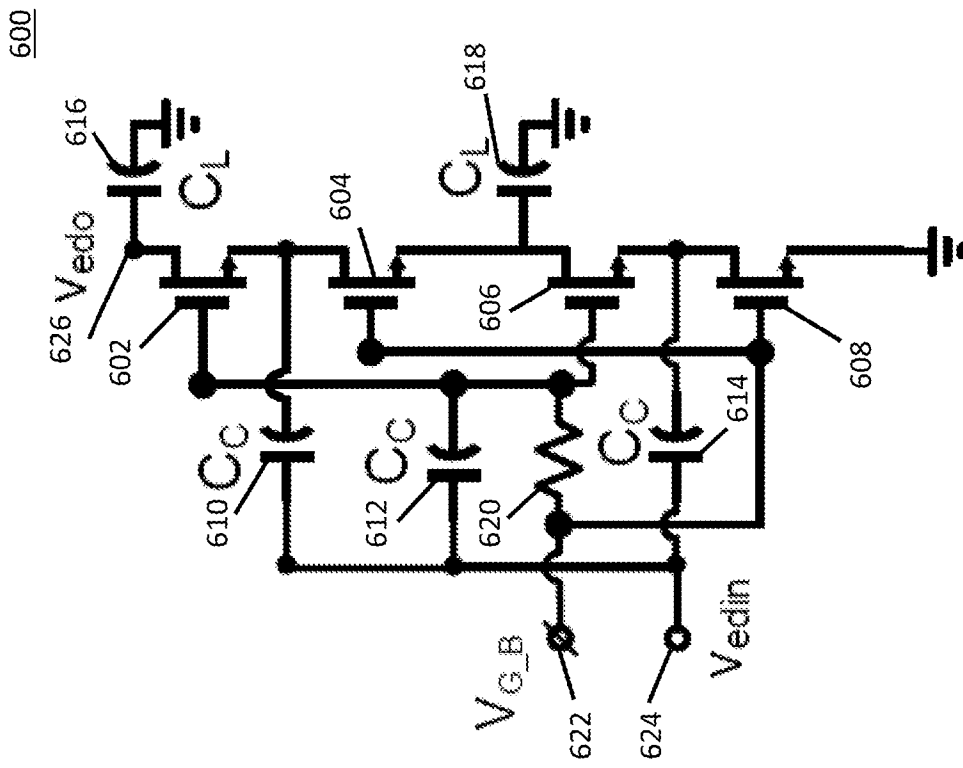


FIG. 6A

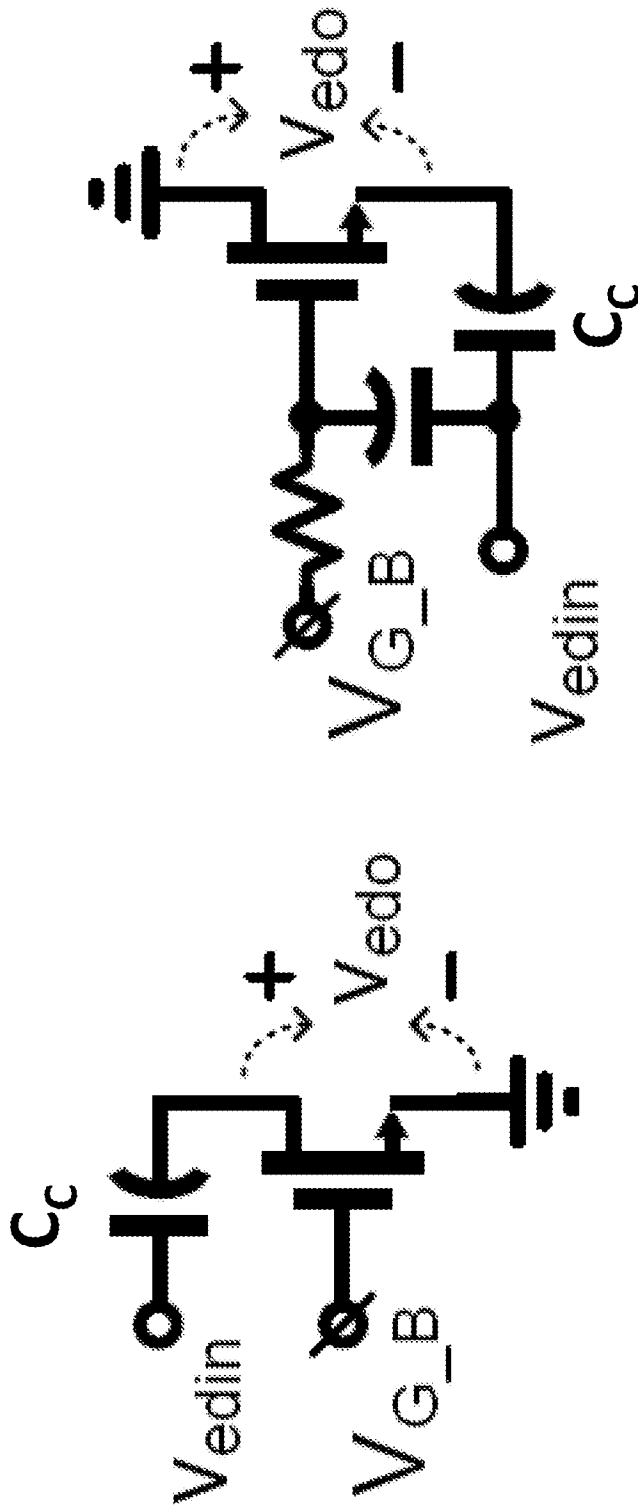


FIG. 6C

FIG. 6B

Small-signal model @ RF input

Small-signal model @ baseband output

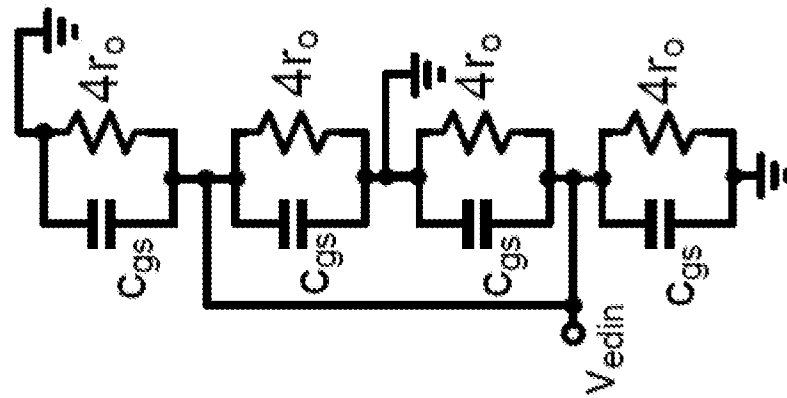


FIG. 7A

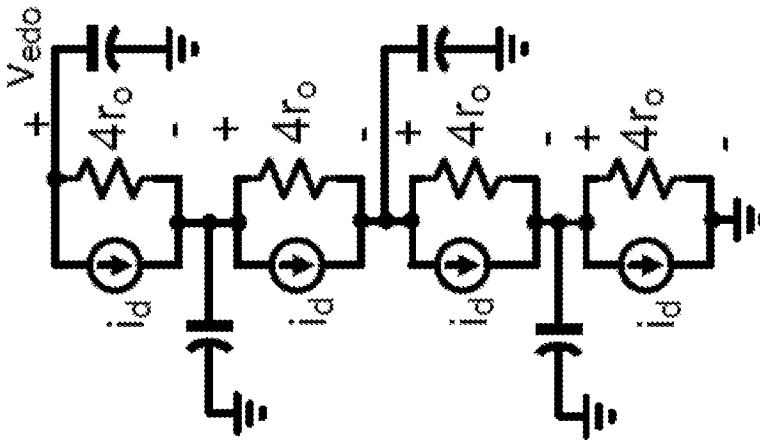


FIG. 7B

10/29

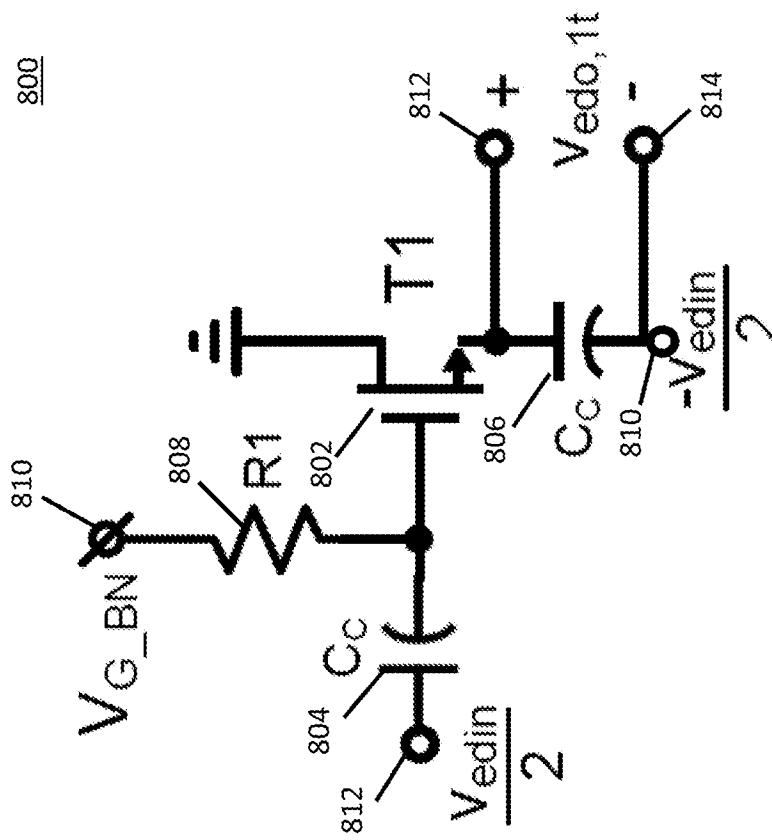


FIG. 8

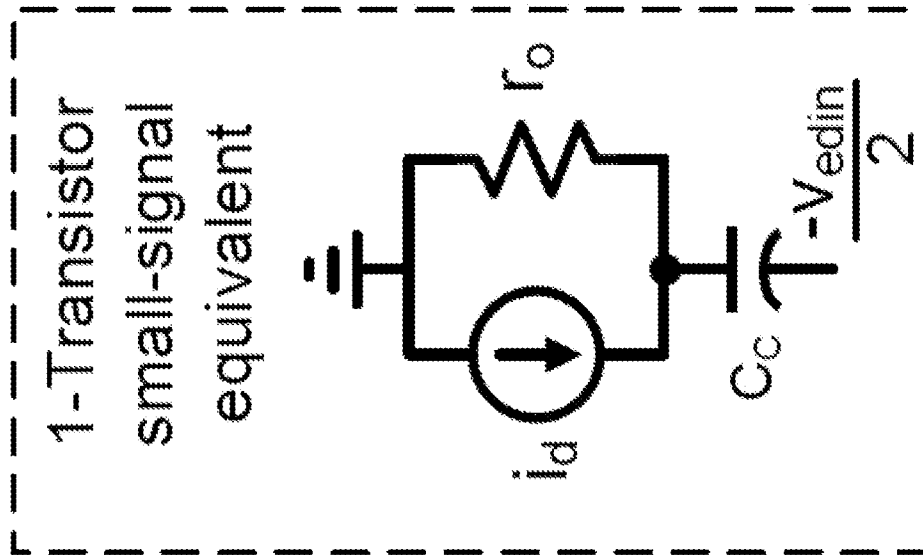
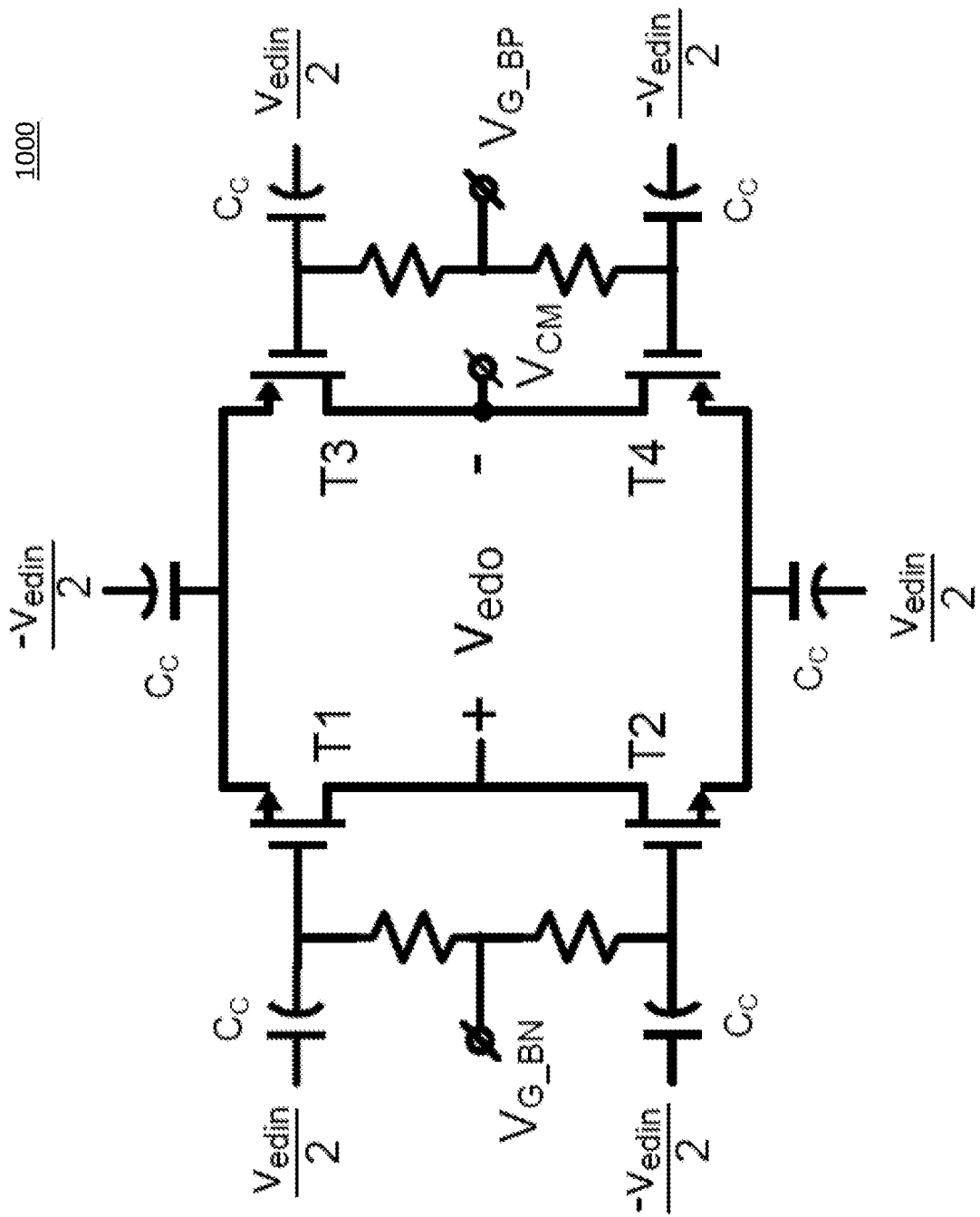


FIG. 9

12/29



1000

FIG. 10

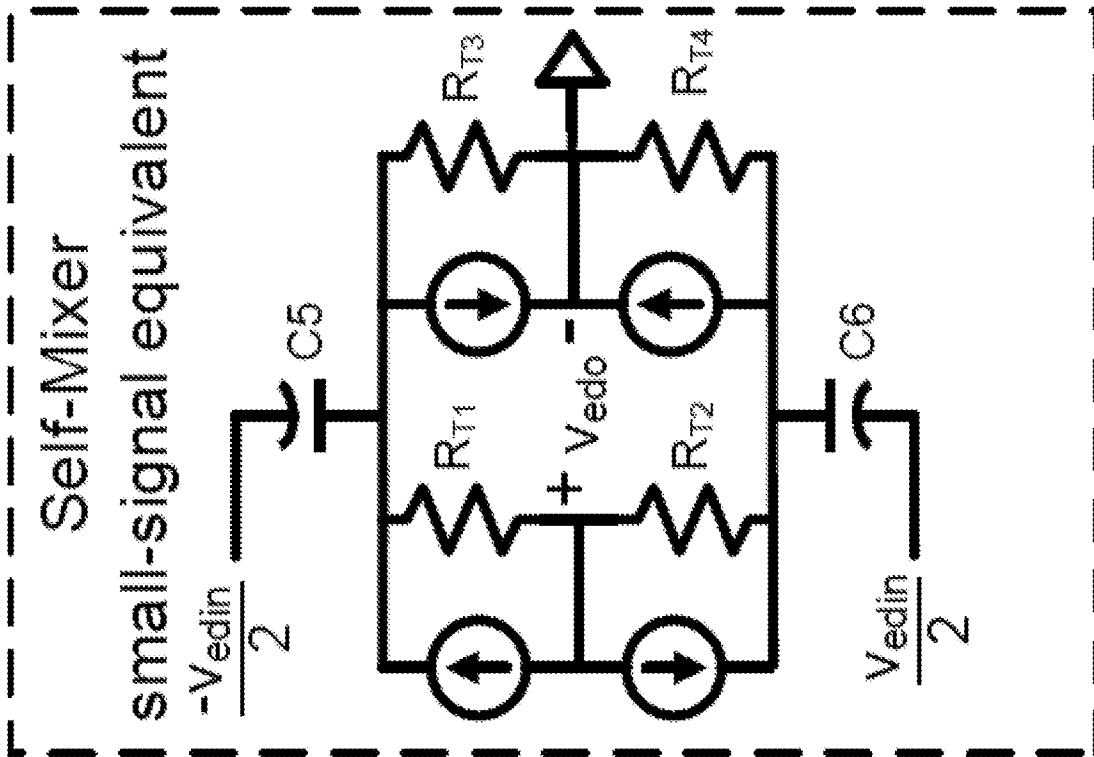


FIG. 11

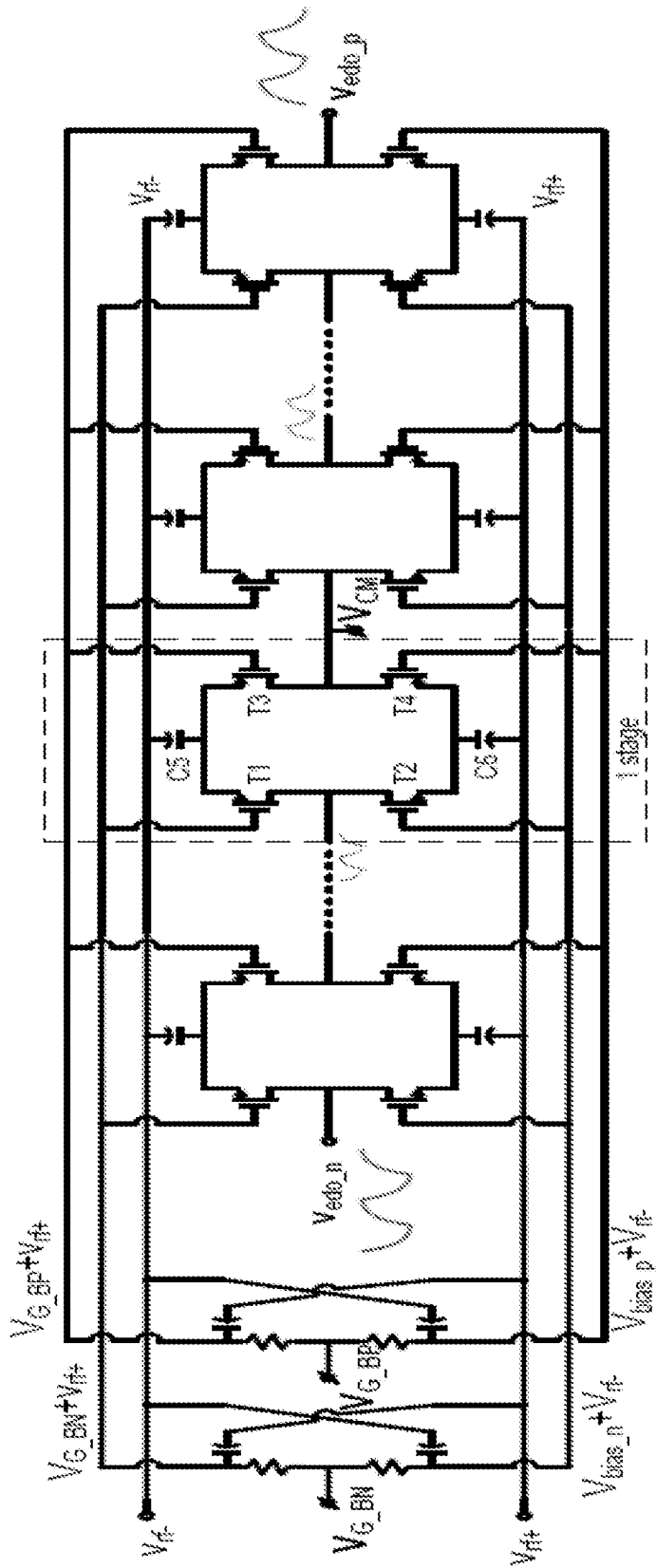


FIG. 12

1400

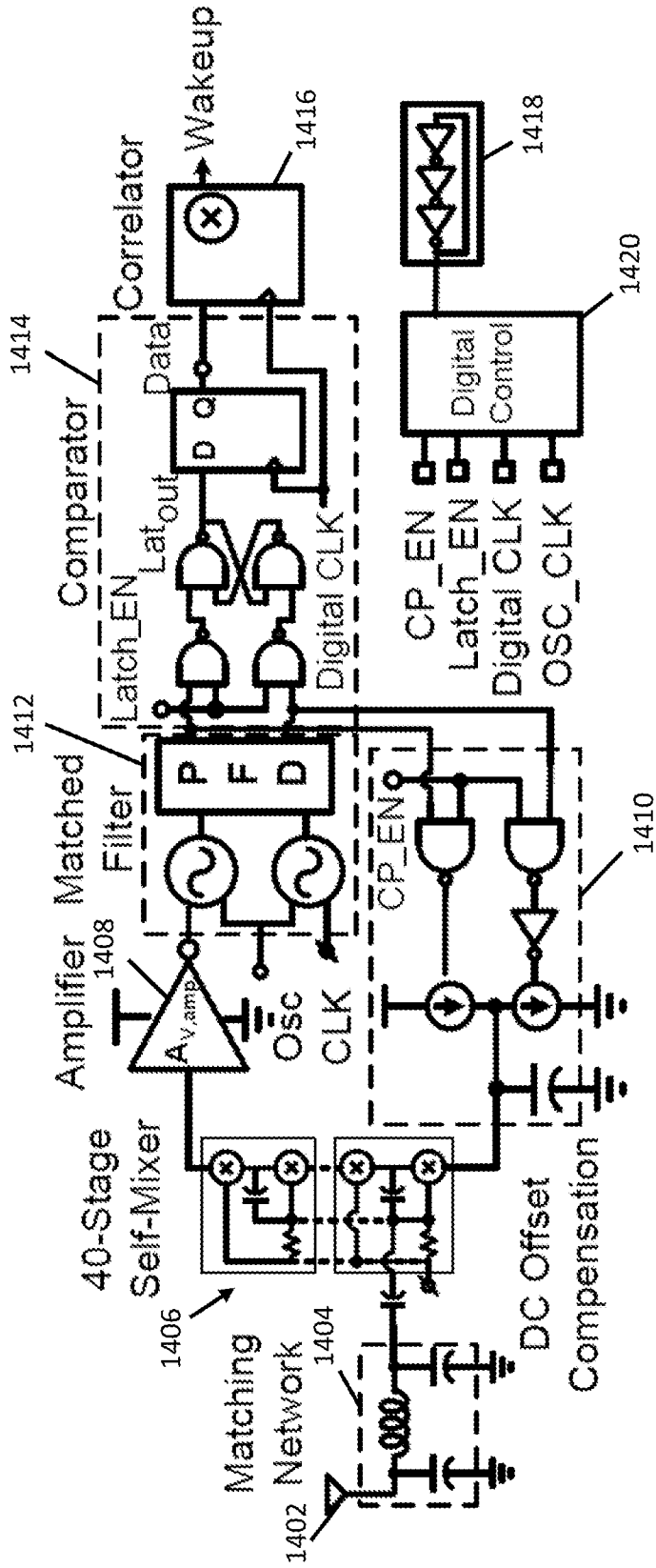


FIG. 14

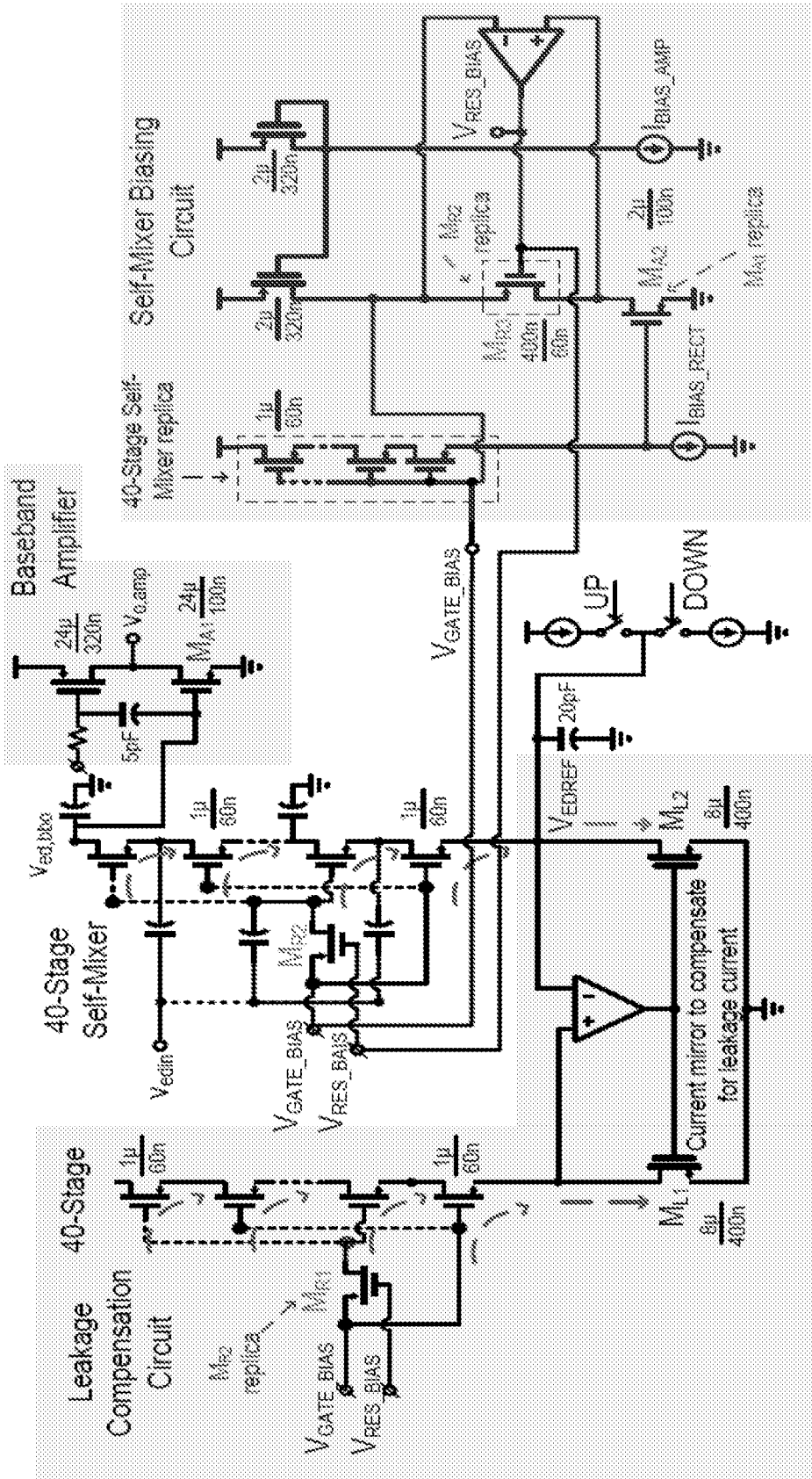


FIG. 15

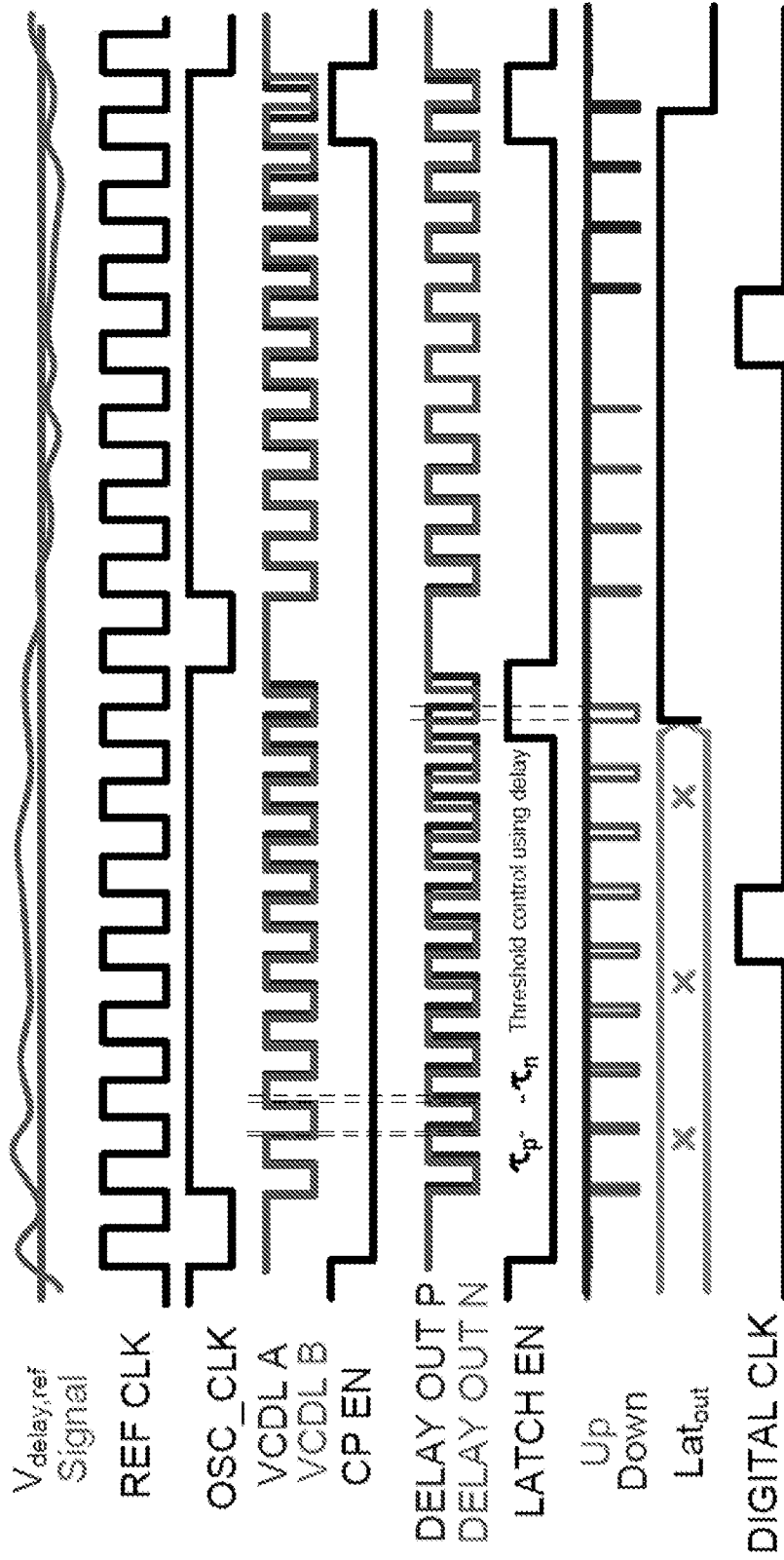


FIG. 17

1900

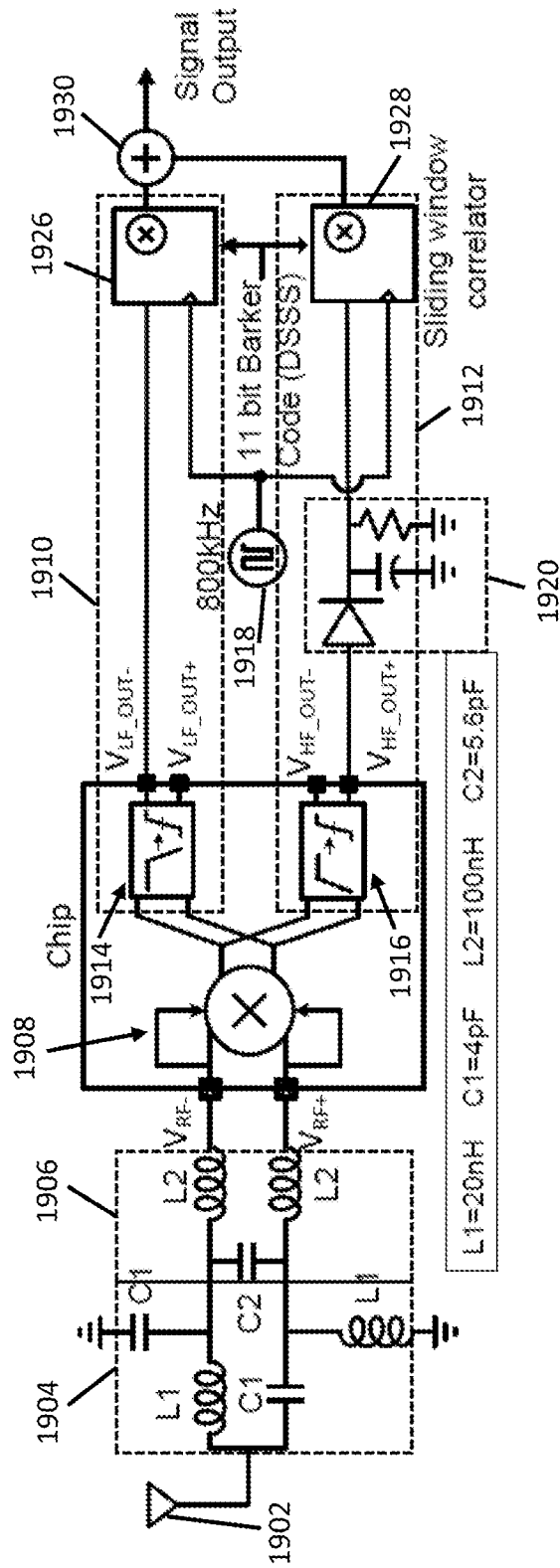


FIG. 19

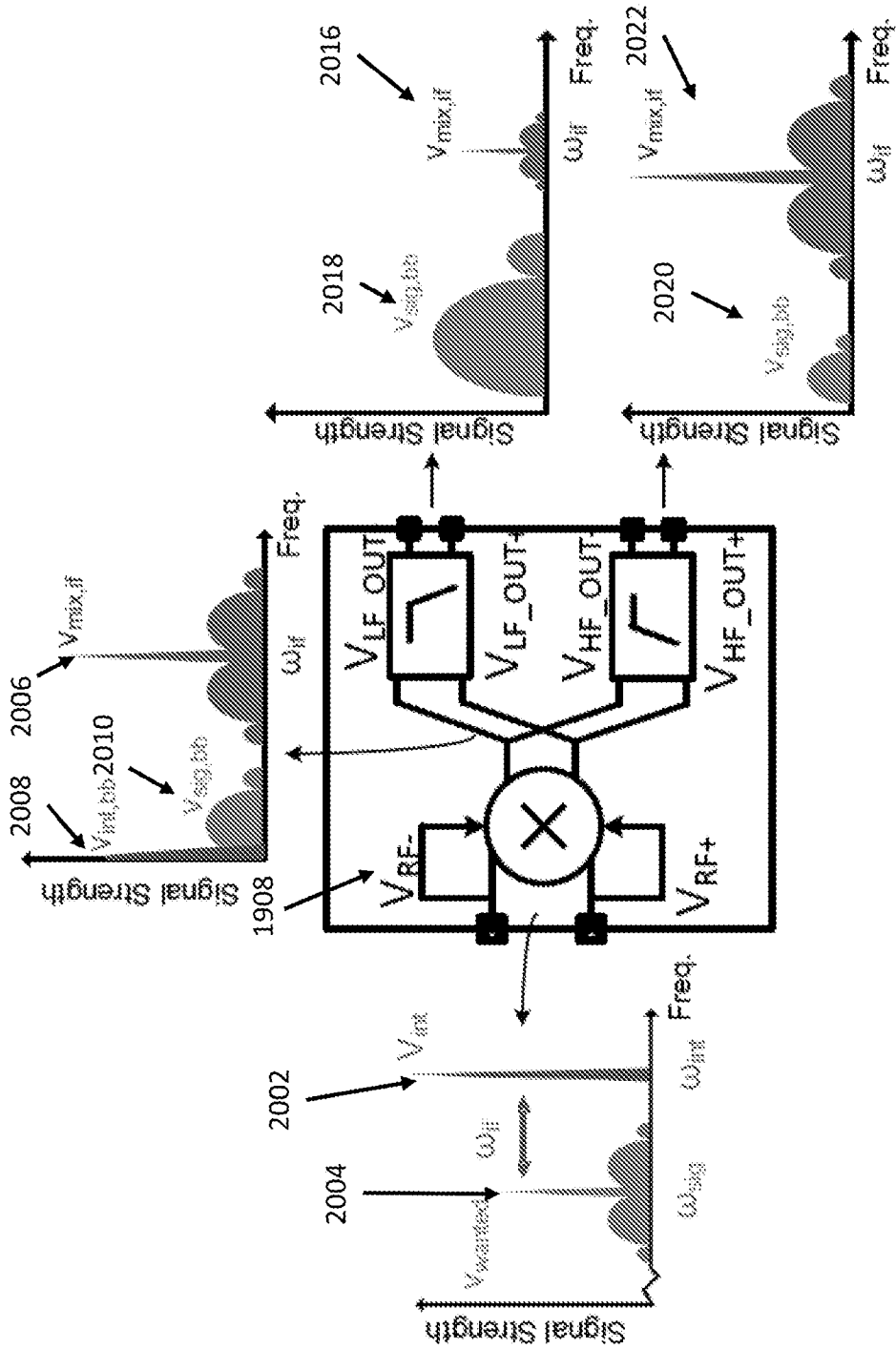


FIG. 20

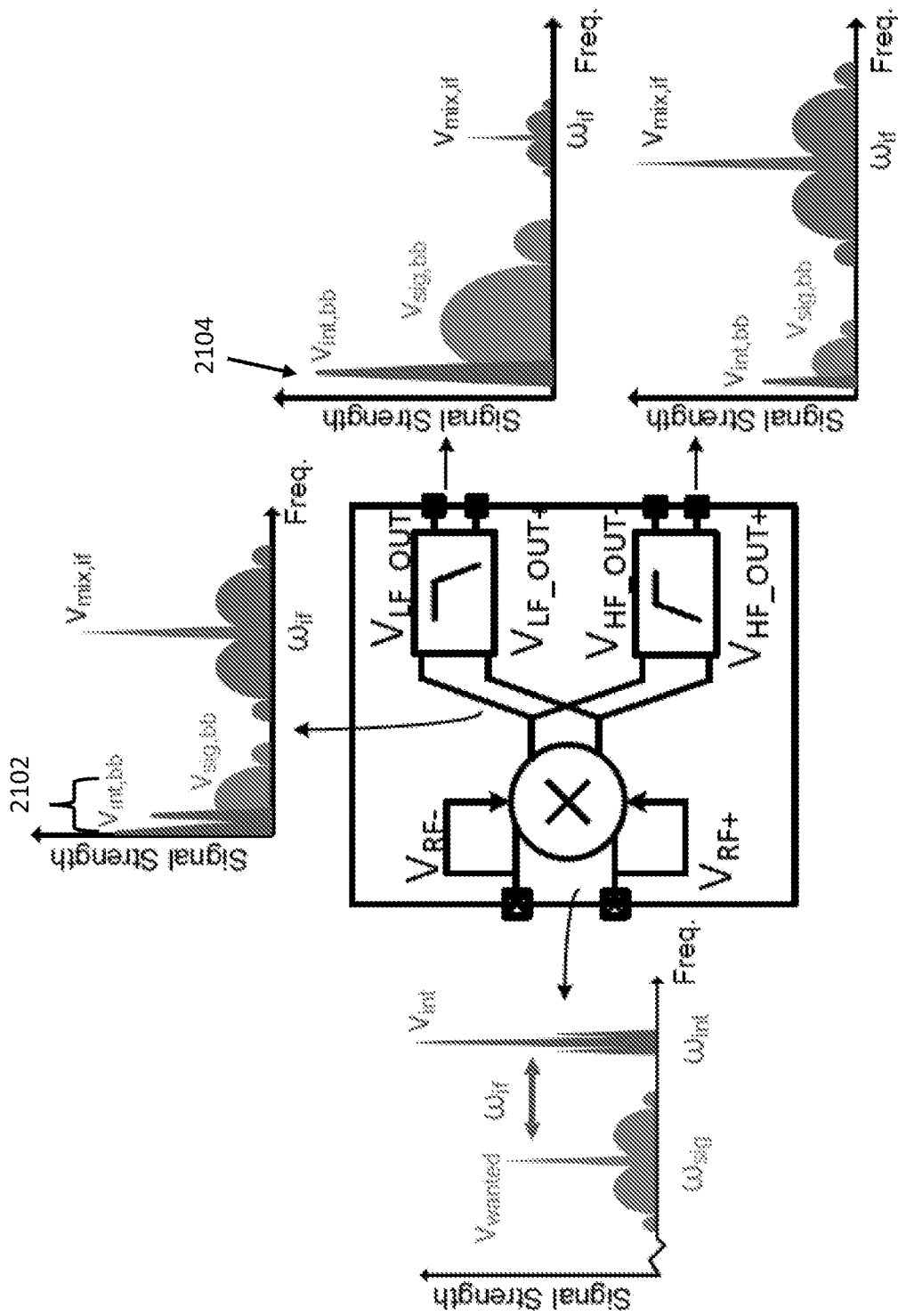


FIG. 21

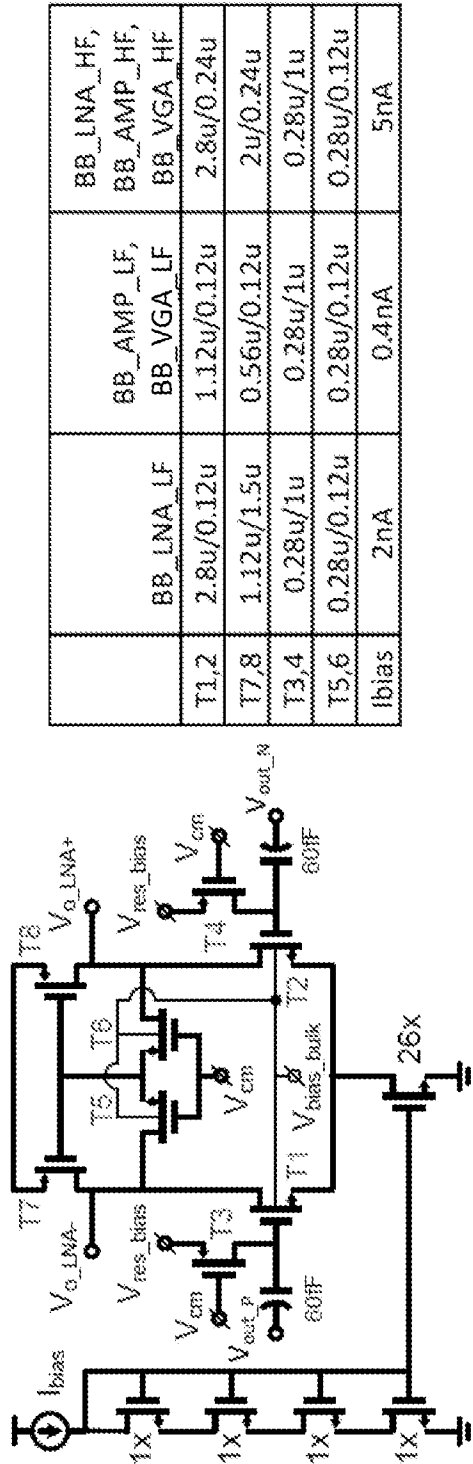


FIG. 24

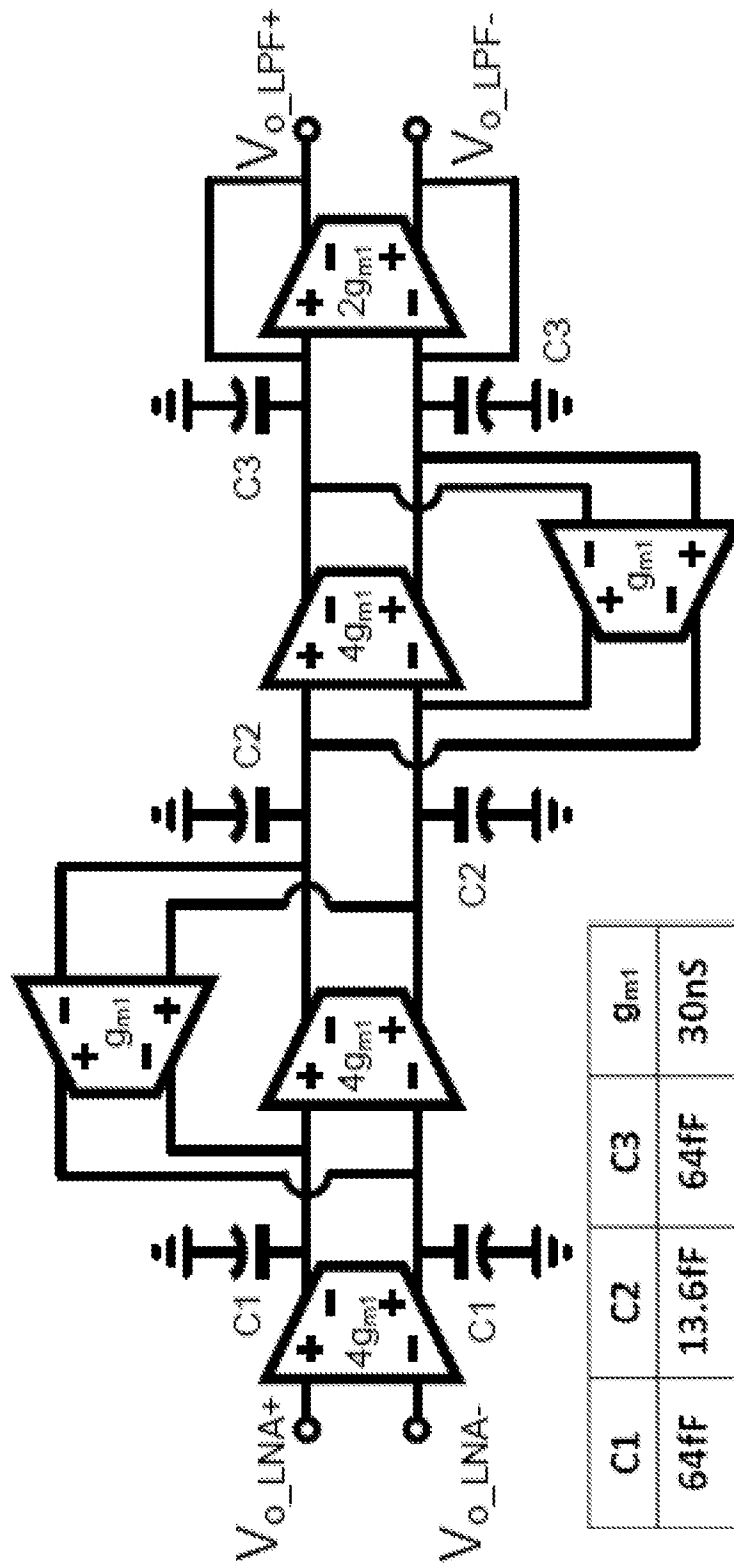


FIG. 25

INTERNATIONAL SEARCH REPORT

International application No.

PCT/US 20/12439

A. CLASSIFICATION OF SUBJECT MATTER
 IPC - H04B 1/16; H04L 27/06; H04W 52/02 (2020.01)
 CPC - H03D 7/1466; H04B 1/16; H04L 27/06; H04W 52/0229; Y02D 70/00

According to International Patent Classification (IPC) or to both national classification and IPC

B. FIELDS SEARCHED

Minimum documentation searched (classification system followed by classification symbols)
 See Search History document

Documentation searched other than minimum documentation to the extent that such documents are included in the fields searched
 See Search History document

Electronic data base consulted during the international search (name of data base and, where practicable, search terms used)
 See Search History document

C. DOCUMENTS CONSIDERED TO BE RELEVANT

Category*	Citation of document, with indication, where appropriate, of the relevant passages	Relevant to claim No.
P, X	MANGAL et al., "A Wake-Up Receiver With A Multi-Stage Self-Mixer and With Enhanced Sensitivity When Using an Interferer as Local Oscillator." IEEE Journal of Solid State Circuits. Vol 54 No 3, 04 January 2019 (04.01.2019) [online] <URL: https://ieeexplore.ieee.org/abstract/document/8602362 >	1-17
X --- Y	MANGAL e tal., "An Ultra-Low-Power Wake-Up Receiver with Voltage Multiplying Self-Mixer and Interferer-Enhanced Sensitivity." 2017 IEEE Custom Integrated Circuits Conference (CICC), 27 July 2017 (27.07.2017) [online] <URL: https://ieeexplore.ieee.org/abstract/document/7993615 >	1-14, 16, 17 ----- 15
Y	US 8,611,480 B1 (LEE et al.) 17 December 2013 (17.12.2013) Fig 7, abstract, col 6, ln 64-col 7, ln 15	15
A	US 8,340,623 B2 (LU et al.) 25 December 2012 (25.12.2012) Fig 5, abstract	1-17

Further documents are listed in the continuation of Box C. See patent family annex.

* Special categories of cited documents:	"T" later document published after the international filing date or priority date and not in conflict with the application but cited to understand the principle or theory underlying the invention
"A" document defining the general state of the art which is not considered to be of particular relevance	"X" document of particular relevance; the claimed invention cannot be considered novel or cannot be considered to involve an inventive step when the document is taken alone
"D" document cited by the applicant in the international application	"Y" document of particular relevance; the claimed invention cannot be considered to involve an inventive step when the document is combined with one or more other such documents, such combination being obvious to a person skilled in the art
"E" earlier application or patent but published on or after the international filing date	"&" document member of the same patent family
"L" document which may throw doubts on priority claim(s) or which is cited to establish the publication date of another citation or other special reason (as specified)	
"O" document referring to an oral disclosure, use, exhibition or other means	
"P" document published prior to the international filing date but later than the priority date claimed	

Date of the actual completion of the international search 06 March 2020	Date of mailing of the international search report 01 MAY 2020
Name and mailing address of the ISA/US Mail Stop PCT, Attn: ISA/US, Commissioner for Patents P.O. Box 1450, Alexandria, Virginia 22313-1450 Facsimile No. 571-273-8300	Authorized officer Lee Young Telephone No. PCT Helpdesk: 571-272-4300